# Assessing Tree Carbon Estimates from Remotely Piloted Aircraft-Based LiDAR: A Comparison of Quantitative Structural Models and Allometric Scaling with In-Situ DBH Measurements

by

Chenxi Liu

A thesis

presented to the University of Waterloo

in fulfillment of the

thesis requirement for the degree of

Master of Science

in

Geography

Waterloo, Ontario, Canada, 2024

© Chenxi Liu 2024

# Author's Declaration

This thesis consists of material all of which I authored or co-authored: see Statement of Contributions included in the thesis. This is a true copy of the thesis, including any required final revisions, as accepted by my examiners.

I understand that my thesis may be made electronically available to the public.

# Statement of Contribution

This thesis contains a manuscript journal article that investigates the use of drone-based LiDAR data and Quantitative Structure Models (QSMs) for estimating tree Diameter at Breast Height (DBH) and forest carbon storage. The manuscript is intended for submission to a peer-reviewed journal following the defense of this thesis and will be co-authored with my supervisor, Dr. Derek Robinson. Dr. Robinson provided critical insights into the research framework, suggesting key improvements for the experimental design and offering substantial revisions to the manuscript to ensure clarity and precision in communicating the research findings. My contributions include the conceptualization of the study, the development of the experimental design, execution of the research, data analysis, and drafting of the manuscript. I also acknowledge the contributions of Brandon Giura, who was instrumental in the data acquisition process, particularly in the use of the GNSS receiver for tree location measurements, the collection of ground control points, and point cloud data processing. Mathew Shetler and Erin Gouthro provided valuable assistance in the initial identification of tree species and the measurement of DBH. Anas Alsharo played a key role in the calibration of the TreeQSM model, ensuring the accuracy of the results obtained in this study.

# Abstract

Forest carbon storage estimation is critical for global climate change mitigation efforts, as forests play a vital role in the carbon cycle. This study investigates the accuracy of using Remotely Piloted Aircraft (RPA)-based LiDAR for estimating tree Diameter at Breast Height (DBH) and carbon storage through 3D tree modeling techniques. Two Quantitative Structure Models (QSM) — TreeQSM and AdQSM were used to virtually reconstruct trees and estimate tree and forest carbon stocks, with comparisons made to in-situ DBH measurements and traditional Allometric Scaling Models (ASMs), including self-developed allometric equation database and i-Tree Eco. Data were collected from two forest sites with different tree densities in Ontario, Canada, under leaf-on and leaf-off conditions. Result indicates that AdQSM generally outperformed TreeQSM in estimating DBH, particularly in less dense forests and during leaf-off season, where the correlation with in-situ DBH measurements improved. Despite variation in results from the two models, RPA-based LiDAR demonstrated potential as a scalable and non-destructive tool for forest carbon estimation, providing a foundation for future advancements in localized ASMs. The findings highlight the importance of accurate tree parameter extraction for forest carbon accounting, aligning with global efforts in climate change mitigation and sustainable forest management.

# Acknowledgements

First, I would like to thank my committee members, Dr. Derek Robinson, Dr. Andrew Trant, and Dr. Grant Gunn, for their support and guidance to this thesis.

I have always considered myself a fortunate person, in many aspects of life.

As a student, I have been incredibly lucky. I had the opportunity of learning from the very best, my advisor Dr. Derek Robinson—without a doubt, the coolest and most professional mentor I could have asked for. Your impact on me extends far beyond academia. Your boundless energy, your relentlessly positive attitude toward both life and work—these are qualities I will continue to strive for. You are my role model.

I'm also a lucky child, blessed with the unconditional love of my parents, Dong Xue and Yongbo Liu, and my grandparents, Changxiang Xue and Ailing Sun. You've always given me the very best of everything. But more than that, you've had the courage to let go—to allow me to explore this vast world freely. Your unwavering support and trust have been my foundation, enabling me to go farther than I ever imagined

I'm super fortunate to have met my dearest friends. To my best friend Yuou (Shirley) Shu, what a blessing it has been to have you by my side in this new chapter of life in a foreign country. I never had to imagine what the best version of friendship could look like, because I've experienced it with you. To my amazing "big brother" Brandon Giura, thank you for making every fieldwork outing a joy—adventures were always better with you around. And to Renan Cai and Lingfei Ye, thank you for being my guides through the early days of journey in this country. Without you, I would have taken far more wrong turns—literally and figuratively.

Lastly, I want to say something to myself, "The most extraordinary sights of the world often lie in perilous and faraway places, where few dare to tread. Only those with ambition can reach them." Keep pushing forward. Keep loving life. Be brave and keep being an adventurer.

# Table of Contents

List of Figures ..... vii
List of Tables ..... viii
**Chapter 1 Introduction ..... 1**
1 Background ..... 1
2 Thesis structure ..... 1
3 Methods for aboveground biomass estimation ..... 2
3.1 Destructive methods ..... 2
3.2 Non-Destructive methods ..... 3
3.2.1 Taper Equations ..... 3
3.2.2 Allometric equations ..... 4
3.2.3 3D Reconstruction ..... 5
**Chapter 2 Main Paper ..... 9**
1 Introduction ..... 9
2 Method ..... 11
2.1 Study site ..... 11
2.2 In-situ sampling ..... 13
2.3 Remotely Piloted Aircraft sampling ..... 14
2.4 Biomass estimation methods ..... 14
2.4.1 Allometric Scaling Model ..... 16
2.4.2 Three-Dimensional (3D) Reconstruction ..... 17
2.4.3 QSM Calibration ..... 20
3 Results ..... 21
3.1 QSM Validation ..... 21
3.1.1 Leaf on versus Leaf off ..... 21
3.1.2 Harvested versus Undisturbed sites ..... 23
3.1.3 DBH Class ..... 25
3.2 Carbon ..... 27
3.2.1 Leaf on versus Leaf off ..... 27
3.2.2 Harvested versus Undisturbed Forest ..... 30
3.2.3 DBH class ..... 33
4 Discussion ..... 34
4.1 Validation ..... 34
4.2 Carbon ..... 36
4.3 Future Avenues for Investigation ..... 38
5 Conclusion ..... 39
**Chapter 3 Future Work ..... 41**
**References ..... 44**

# List of Figures

Figure 1. Study area. ..... 12

Figure 2. Workflow ..... 15

Figure 3. DBH distributions in leaf-on and leaf-off season. ..... 23

Figure 4. DBH distribution by study site for Harvested and Undisturbed forests ..... 25

Figure 5. DBH class distributions in leaf-on and leaf-off conditions. ..... 27

Figure 6. Carbon storage distribition in leaf-on and leaf-off conditions. ..... 30

Figure 7. Carbon storage distribution by study sites for Harvested and Undisturbed forests. ..... 32

Figure 8. Carbon storage distribution by DBH class in leaf-on and leaf-off conditions. ..... 34

Figure 9. Comparison of 3D reconstruction models with LiDAR data under different data quality conditions. ..... 36

# List of Tables

Table 1. Overview of modern taper equation types ..... 3

Table 2. Overview of representative allometric equation databases ..... 4

Table 3. Comparison of Tree Modeling algorithms ..... 8

Table 4. Summary of in-situ and DBH estimation and accuracy results for TreeQSM and AdQSM in Harvested and Undisturbed forest sites during leaf-on and leaf-off seasons ..... 22

Table 5. Summary of in-situ DBH Class measurements and TreeQSM and AdQSM DBH estimates during leaf-on and leaf-off conditions. ..... 26

Table 6. Summary of carbon storage estimation result from Allometric Scaling Models and QSMs in Harvested and Undisturbed forest sites during leaf-on and leaf-off seasons. ..... 28

# Chapter 1

# Introduction

## 1 Background

Forest is one of the most critical carbon sinks in terrestrial ecosystems, playing a vital role in the global carbon cycle (Malhi et al., 2002). Trees absorb carbon dioxide from the atmosphere and convert it into solid organic matter through photosynthesis, which is then stored within the biomass of trees, woody debris and soil (T. Vashum, 2012). It is estimated that approximately 86% of terrestrial aboveground carbon and 73% of the Earth's soil carbon is sequestered in forested ecosystems (Rodger, 1993).

The types of storage areas for carbon are often referred to as 'pools'. In terrestrial ecosystems five carbon pools are often used to quantify carbon stocks: aboveground biomass, below-ground biomass, dead mass of litter, woody debris, and soil organic matter (IPCC, 2006). Among these pools, aboveground biomass — the total mass of living organic matter in the aboveground portions of trees, is a significant component of terrestrial carbon pools. It constitutes a major portion of the forest's carbon stock and is closely connected to human activities such as land-use change or forest degradation directly impact the carbon pool (T. Vashum, 2012). Therefore, accurately estimating aboveground biomass is crucial for assessing the ecological benefits of forests, monitoring changes in forest carbon storage, and understanding its role in the atmospheric carbon cycle.

In estimating forest carbon stocks, a common approach is to first assess the aboveground biomass and then multiply it by a carbon concentration factor to obtain the final estimate. The most widely recognized biomass-to-carbon conversion factor is 50% for woody tissue (Houghton, 1996) and 45% for foliage and fine roots (Gower et al., 2001). However, the mass-based carbon content varies significantly across different tree species (Zhang et al. 2009). In a study of ten temperate tree species in northeastern China, the carbon content ranged from 49.9 ± 1.3% for stems to 51.4 ± 1.0% for foliage. Similarly, Losi et al. (2003) investigated mixed-species plantations in Panama and found that the carbon content of dry bole samples for *Anacardium excelsum* and *Dipteryx* was 47.8% and 48.5%, respectively.

## 2 Thesis structure

This thesis brings together content from remote sensing and forestry in an effort to improve our ability to quantify above ground tree carbon. While this has been an area of scientific exploration and commercial and industry application for over a century, the role of forests in the global carbon cycle (at a broad scale) and local efforts to quantify natural assets or infrastructure are motivating improvement in tree and forest carbon stock accuracy. This chapter (Chapter 1) reviews the global

significance of forests in the carbon cycle but is primarily focused on introducing different methods used to estimate tree or forest carbon stocks.

The second chapter of the thesis (Chapter 2) is composed as a manuscript for submission to an a yet to be determined academic journal. Chapter 2 describes a comparative analysis of two Quantitative Structure Models (TreeQSM and AdQSM) used for 3D reconstructing tree structure. This Chapter details the methodology of using RPA-based LiDAR to estimate tree Diameter at Breast Height (DBH) and forest carbon storage, also compare these estimates to in-situ measurements and other traditional methods like Allometric Scaling Models. The research goal is to assess the accuracy of RPA-based 3D modeling approaches in estimating forest structural parameters and carbon storage. Specific objectives include evaluating the performance of TreeQSM and AdQSM in diverse forest conditions, quantifying their estimation accuracy against in-situ measurements, and investigating how these models perform in the carbon stock estimation.

It should be noted that while I conducted the majority of research and writing in Chapter 2 that several individuals assisted with the research. In addition to my supervisor Dr. Derek Robinson's assistance, Brandon Giura assisted with GNSS receiver data acquisition for tree locations and ground control points and point cloud data processing, Mathew Shetler and Erin Gouthro assisted with initial tree identification and DBH measurements, and Anas Alsharo assisted with the calibration of TreeQSM.

Finally, Chapter 3 notes several broader implications of the research presented in Chapter 2 and situates it within the global context of climate change mitigation and sustainable forest management.

# 3 Methods for aboveground biomass estimation

Estimating tree biomass is challenging due to the complex nature of tree stem form (Temesgen et al., 2015). Currently, there are two conceptual approaches to measure tree biomass, the first involves logging the aboveground components of the tree and weighing them, and the second involves estimating the stem volume and multiplying it by the wood density. Wood density is typically measured by extracting a small sample of stem discs, a few centimeters in size, and determining its volume through water immersion or by measuring its diameter and thickness. The sample is then oven-dried and weighed to obtain the basic density of the wood, usually expressed in $g/cm^3$. Alternatively, increment borer can be used to extract a core of wood from the tree for this purpose (West, 2015). These methods for obtaining biomass or volume are broadly classified into two categories based on whether they require felling the tree: destructive methods and non-destructive methods.

### 3.1 Destructive methods

The destructive method, also known as the harvest method, is the most direct and traditional approach for estimating aboveground carbon storage in trees. This method typically involves selecting and harvesting a representative tree within a sample plot — one that exhibits typical

growth patterns and a regular shape. The tree is then divided into various components, such as the trunk, crown, and foliage. Depending on the desired information, the tree components may be oven-dried and weighed to obtain their mass or subjected to water displacement techniques or xylometry to determine their volume. Although this method is currently the most reliable established method for biomass estimation (Stovall et al., 2018), it is time-consuming and resource intensive. The limitations in sample size and area, along with the method's destructive nature, make it unsuitable for forests containing species at risk and incompatible with sustainable development principles. Consequently, its application is generally restricted to small-scale studies focused on specific tree species (Weiskittel et al., 2015).

### 3.2 Non-Destructive methods

Given the numerous limitations of the destructive method, its widespread application is impractical, particularly when estimating the carbon stock of large-scale forests (Weiskittel et al., 2015). Species-specific quantitative relationships are often established by correlating key tree growth parameters (e.g., DBH, tree height) with stem volume or mass, which is typically obtained through destructive methods. This approach is commonly used to develop taper equations and allometric equations.

With the advent of Light Detection and Ranging (LiDAR) technology, the tree structure that once required extensive manual measurements can now be represented and stored as point cloud data. These data can be used to create 3D reconstructions of tree stems and branches, allowing for volumetric estimation using a variety of different approaches.

#### *3.2.1 Taper Equations*

*Table 1. Overview of modern taper equation types and their representative characteristics (McTague & Weiskittel, 2021).*

| Name | Representative Works | Equation Example | Features |
|---|---|---|---|
| Variable-form | Newnham (1992); Kozak (1988, 2004) | $d_u = a_0 DBH^{a_1} H^{a_2} X^{\left(b_1 z^4 + \frac{b_2}{e^{\frac{DBH}{H}}} + b_3 X^{0.1} + \frac{b_4}{DBH} + b_5 H^Q + b_6 X\right)}$ | Highly flexible and robust across multiple species; requires numerical integration for volume estimates; may have high multicollinearity. |
| Compatible | Demaerschalk (1972); Fang et al. (2000); Sharma and Oderwald (2001) | $d_u^2 = DBH^2 \left(\frac{h_u}{1.3}\right)^{2-y} \left(\frac{H - h_u}{H - 1.3}\right)$ | Ensures consistent linkages between stem form and volume; can be algebraically integrated; may reduce flexibility with limited accuracy improvement. |
| Polynomial/ Segmented/ Splines | Kozak et al. (1969); Goodwin (2009); Téo et al. (2018) | $\frac{d_u}{DBH} = 1.149 - 3.4350 \times \left(\frac{h_u}{H}\right) + 16.0934 \times \left(\frac{h_u}{H}\right)^2 - 38.7426 \times \left(\frac{h_u}{H}\right)^3 + 40.4870 \times \left(\frac{h_u}{H}\right)^4 - 15.5778 \times \left(\frac{h_u}{H}\right)^5$ | Simple to fit and apply; can overfit and not extrapolate well; segmented models ensure proper behavior but can be challenging to determine optimal points. |
| Trigonometric/ Matrix | Matney et al. (1985); Thomas and Parresol (1991) | $\frac{h_u}{H} = 1 - \left\{1 - e^{-a \times tan\left[b \times H^c \times \left(\frac{d_u}{DBH}\right)\right]}\right\}^d$ | Flexible and parsimonious; robust for species with complex forms; may reduce flexibility and can be inconsistent in behavior. |

The basic principle of the taper function is to conceptualize the tree as a combination of geometric shapes (e.g., cylindrical, parabolic, and conical). Using mathematical formulas, the taper function

estimates how the stem diameter changes from the base of the tree to its tip. The application of taper equations dates back to the late 1800s and over more than a century of development taper equation forms have evolved into four main types: 1) variable form; 2) compatible and parsimonious; 3) polynomial, segmented, and splines; 4) trigonometric and matrix (McTague & Weiskittel, 2021)

*3.2.2 Allometric equations*

The allometric equation, also known as the biomass estimation equation, is a method used to estimate the aboveground biomass or volume of a tree based on its Diameter at Breast Height (DBH) and sometimes tree height. The equation is typically established using destructive methods, which involve weighing or measuring the volume of specific tree species and then establishing a mathematical relationship between these measurements and the tree's DBH and height. Generally, the relationship between individual tree biomass and stem volume is represented by an equation such as (x).

$$Y = \beta_0 {X_1}^{\beta_1} {X_2}^{\beta_2} \dots {X_j}^{\beta_j} + \varepsilon \quad (1)$$

In which, Y is tree biomass (kg) or volume ($m^3$); $X_j$ is tree growing variables (e.g. DBH, tree height., etc); $\beta_j$ are coefficient and $\varepsilon$ is error term.

*Table 2. Overview of representative allometric equation databases*

| Database | Equation form | Feature | Citation |
|---|---|---|---|
| Biomass equations for sixty-five North American tree species | $Biomass = a \times DBH^b$ | Contains 803 equations and presents biomass equations for 65 North American tree species. Equations for total aboveground biomass, stem wood, stem bark, and other tree components are also included. | Ter-Mikaelian & Korzukhin, 1997 |
| Updated generalized biomass equations for North American tree species | $\ln(Biomass) = a + b \times ln(DBH)$ | Presents 35 generalized biomass equations, divided among 13 conifer, 18 hardwood, and 4 woodland taxa for North American tree species. These equations were developed using a comprehensive meta-analysis of 3,464 biomass equations from 206 sources. | Chojnacky et al., 2014 |
| Urban tree database and allometric equations | $Biomass = a \times DBH^b$<br>$Biomass = a \times DBH^b \times H^c$ | Records 365 sets of allometric equations that were developed based on 14,487 urban street and park trees across 17 U.S. cities. These equations cover 171 distinct species, representing urban trees | McPherson, 2016 |
| Weight-diameter relationships for 22 woody plant species | $\log(Biomass) = a + b \times log(DBH)$ | Collects prediction equations for the total aboveground and leaf weights of 22 woody plant species in Canada, using stem diameter at the ground line as the primary predictor in a log-linear format | Telfer, 1969 |

The various widely used allometric equations have evolved from the basic formula (Eq. 1) and are typically transformed into polynomial or logarithmic forms to facilitate calculation. Table 2 provides an overview of several allometric equation databases, including their key characteristics and forms.

The scientific literature on allometric equations is often fragmented, with most studies focusing on a specific stand or a few tree species. When the scope expands to cover landscape-level, incorporating allometric equations from different source scan become a required and cumbersome task (Ter-Mikaelian & Korzukhin, 1997). To address this issue, Allometric Scaling Models (ASMs) were developed, incorporating species-specific, localized allometric equations that cover one or more natural regions. ASMs not only function as a comprehensive database but also include internal calculation mechanisms. Based on tree inventory data, they automatically input tree growth parameters into the equations to estimate tree biomass, carbon storage, and other ecosystem services. More importantly, compared to traditional allometric equations, some ASMs incorporate the effect of human-induced or natural disturbance. For example, i-Tree Eco can adjust the estimated ecosystem services based on the tree's location, proximity to buildings, and natural disturbances. Representative ASMs include i-Tree Eco and the Carbon-Budget Model of the Canadian Forestry Service (CBM-CFS).

i-Tree Eco (https://www.itreetools.org/), developed by the United States Department of Agriculture Forest Service (USDAFS), is a model designed to comprehensively understand the ecosystem benefits of urban forest structures. It assesses vegetation structure, function, and carbon value. The primary application method involves users inputting urban forest inventory data into i-Tree Eco, which estimates tree characteristics such as forest cover, leaf area, carbon storage and sequestration, oxygen production, and other ecosystem services. Initially applied to major cities in the United States, i-Tree Eco's reach has since expanded globally. Nowak et al. (2013) used i-Tree Eco to assess urban tree carbon storage across 28 cities in six U.S. states, estimating a national average of 7.69 kg C/m². Kim et al. (2024) employed i-Tree Eco in Yurim Park, Daejeon, South Korea, and found that the total carbon storage in the park ranged from 0.5 to 2.14 kg C/m², with an average of 1.53 kg C/m² across the area. This flexibility allows i-Tree Eco to be applied on both large national scales and smaller, localized areas such as parks.

The Carbon Budget Model (CBM), developed by the Canadian Forest Service (CFS), is an inventory-based model aimed at estimating above- and below-ground biomass and the dynamics of forest carbon stocks, including dead wood and soil organic carbon. CBM follows the methodological guidance set by the Intergovernmental Panel on Climate Change (IPCC, 2003, 2006). Unlike some other empirical models (e.g., CO2Fix V.2, EFISCEN) that overlook or simplify the impacts of silvicultural systems and natural disturbances, CBM-CFS3 integrates both natural and human-induced disturbance effects (Kull et al., 2006; Kurz et al., 2008). The model supports stand- and landscape-level carbon modeling and has been successfully applied at national and regional scales in Canada (Kurz et al., 2009; Amichev et al., 2016), Russia (Zamolodchikov et al., 2008), and Italy (Pilli et al., 2013).

*3.2.3 3D Reconstruction*

Accurate and fast acquisition of individual tree parameters is the most critical yet challenging step in forest biomass modeling. The previously mentioned taper equation and allometric equation

modelling approaches are developed based on known tree growth parameters through fitting processes. The advantage of 3D reconstruction lies in its ability to integrate automatic individual tree parameter extraction with the estimation of total tree volume, eliminating the need for laborious fieldwork and the subsequent effort of matching collected data to corresponding equations. Establishing a 3D forest model requires the use of remote sensing tools such as Light Detection and Ranging (LiDAR) or digital aerial photogrammetry. LiDAR can capture high-density point cloud data of trees, and by mounting LiDAR sensors on various remote sensing platforms such as terrestrial laser scanning, airborne laser scanning, or Remotely Piloted Aircraft system (RPAS) laser scanning, one can acquire LiDAR data of varying density and scope depending on the need. Similarly, image-based remote sensing tools can also obtain 3D point cloud data and build accurate 3D forest models (Zhu et al., 2021).

Regardless of the tool used, acquiring 3D point clouds is the key to enabling automatic tree extraction. 3D reconstruction utilizes 3D point clouds to create a three-dimensional model that best fits the tree structure. Depending on the fitting method or statistical approach, the most widely applied 3D reconstruction methods can be categorized into three types: voxel-derived models (Hosoi et al., 2013; Bienert et al., 2014), stem curve models (Kankare et al., 2013; Liang et al., 2016), and quantitative structure models (Raumonen et al., 2013, Raumonen et al., 2015, Brede et al., 2019).

**Voxel-derived model**

Voxelization is an innovative approach in 3D reconstruction, has gained significant traction in various fields, especially in forestry (Sumnall et al., 2016). This technique involves converting 3D space into a grid of cubes known as voxels (volumetric pixels), simplifying the complex branching patterns of tree point clouds into more digestible volumetric sections and facilitating detailed analysis (Stovall et al., 2017) and modeling complex forest structures. LiDAR, especially terrestrial LiDAR data, has shown remarkable strides in tree volume estimation using voxel-based methods.

Building on the fundamental concepts of Aboveground Biomass estimation, the pioneering work of Hauglin et al. (2013) showcases the application of voxelization in estimating the branch biomass of Norway spruce trees using TLS. In this study, the voxel-based model based on 0.4 m voxel data provided the best prediction accuracy, with a Root Mean Square Error (RMSE) of 32%, highlighting the potential of voxel-based approaches in the estimation of tree biomass, particularly in improving the accuracy of biomass estimations compared to traditional allometric models. Hosoi et al. (2013) refined the methodology by crafting a 3D voxel-based model with portable scanning lidar, bypassing the need for traditional allometric equations and shape assumptions. Additionally, this study highlighted the versatility of voxelization in dealing with diverse tree types, thus broadening the scope of its usage in forestry. Bienert and Hess (2014) emphasized the importance of voxel size in the accuracy of biomass estimations, shedding light on how different voxel dimensions can influence the outcome of the analysis and finding that smaller voxel sizes more accurately represented the tree volume. This insight into voxel size is crucial for optimizing

voxelization methodologies and influencing decisions on data resolution and processing strategies in forestry applications.

**Stem Curve Model**

In Section 3.2.1, we introduced the taper equation, also known as the stem curve, which mathematically describes the diameter variation of a tree from the stump to the top. The most accurate way to develop a stem curve is through the use of a logging machine, which cuts the stem at regular intervals to obtain the diameter of each disc, and then estimates the stem volume based on the combined shape of these discs. However, this destructive method lacks general applicability, as it is unsuitable for large-scale biomass assessments or conservation areas. LiDAR-based point cloud data, on the other hand, has the capability to accurately capture the 3D structure of a tree stem. According to Liang et al. (2014), the basic approach to developing a stem curve and estimating stem volume using terrestrial laser scanning (TLS) data is outlined below.

The first step involves capturing the tree stem shape using TLS-based point cloud data. After filtering the point cloud, robust estimation is applied to fit a series of cylinders to the data points. Once the cylinders are consistently aligned to cover the entire tree point cloud, a 3D stem model is constructed, which is then used to fit the stem taper equation. The third step, stem volume estimation, involves calculating the total stem volume from the 3D model. Each section of the stem is treated as a cylindrical segment, and the volume is calculated by summing the volumes of all these segments. The stem volume is computed using a formula that assumes a circular cross-section for each segment.

**Quantitative Structure Model**

Quantitative Structure Modeling (QSM) has become a leading method in forest research for estimating biomass and reconstructing the 3D architecture of trees using point cloud data from LiDAR (Disney et al., 2018). Raumonen et al. (2013) introduced QSM as a geometric model that structures tree components, such as trunks and branches, in a hierarchical manner. Through cylinder-fitting algorithms, QSM uses point cloud data to capture intricate tree details, including trunk and branching patterns, with significant accuracy. This allows researchers to estimate tree volume by summing the cumulative volumes of cylindrical segments. The subsequent step is to calculate biomass by incorporating wood density (Calders et al., 2015; Hackenberg et al., 2015).

The basic approach to QSM involves segmenting point cloud data into large patches (broad segmentation), followed by finer segmentation to capture detailed branching structures (Calders et al., 2015; de Tanago et al., 2018). This segmentation is achieved through a two-step process, where the point cloud is initially divided into uniform patches that identify the tree's general framework. Then, smaller patch diameters are applied to refine the segmentation of the branches, creating a more precise model of the tree's structure.

Since its introduction, QSM has been validated in various forested environments. Studies, such as those by Raumonen et al. (2013) and de Tanago et al. (2018), have shown QSM's reliability across diverse forest types, including tropical ecosystems where complex tree forms pose challenges.

Brede et al. (2019) explored the application of QSM using RPA-LiDAR and showed that QSM could produce accurate DBH estimates, though performance varies based on branch size and forest structure. Lin et al. (2022) also utilized dual-source RPA data (LiDAR and Structure-from-Motion) to estimate urban tree biomass, highlighting QSM's potential for different types of forest environments. Several QSM models have been developed, including TreeQSM, AdQSM and SimpleTree, etc. Each algorithm refines the methodology to account for varying tree morphologies and improve accuracy (Fan et al., 2020; Hackenberg et al., 2015). To provide a clearer comparison of various QSMs and their features, Table 3 lists some of the most commonly used QSMs, including their methodologies, computer languages and citations for further reference.

*Table 3. Comparison of Tree Modeling Software: TreeQSM, AdTree, Simple Tree, PypeTree and AdQSM*

| Software | Year of Release | Methodology Used | Computer Language | Citation |
|---|---|---|---|---|
| TreeQSM | 2014 | Hierarchical collection of cylinders to estimate tree structure details | MATLAB | Raumonen et al. (2013), Calders et al. (2015), Raumonen et al. (2015) |
| AdTree | 2019 | Reconstruction of branches and leaves from point clouds as triangle meshes | C++ | Du et al. (2019) |
| Simple Tree | 2020 | The utilization of spheres to follow the complete branching structure of a tree | C++ | Hackenberg et al. (2015) |
| PypeTree | 2014 | Reconstruction based on skeletal extraction method | Python | Delagrange et al., (2014) |
| AdQSM | 2020 | Representsing a tree as a set of closed and complete convex polyhedra | C++ | Fan et al. (2020) |

The 3D reconstruction models not only provide a non-invasive and accurate means of measuring tree volume and biomass but also eliminate the laborious effort required for fieldwork. By using high-density point cloud data, these models can effectively capture intricate tree structure, such as extraction of DBH and tree volume. As we move forward in this study, the focus will be evaluating these models specifically for estimating tree carbon, considering varying forest conditions and tree growing conditions. The next chapter delves into the methodology and results of assessing tree DBH and carbon estimation using Remotely Piloted Aircraft-based LiDAR and QSM techniques.

# Chapter 2

# Assessing Tree Carbon Estimates from Remotely Piloted Aircraft-Based LiDAR: A Comparison of Quantitative Structural Models and Allometric Scaling with In-Situ DBH Measurements

## 1 Introduction

Forests play a crucial role in the global carbon cycle and the regulation of Earth's climate (Schimel, 2014). Forests are the largest terrestrial aboveground vegetation pool and the degree to which they influence estimates of the North American carbon sink (~1.7 Pg C yr-1 in 1990s, Fan et al. 1998; ~0.65 Pg C $yr^{-1}$ from 2000 to 2005, Peters et al. 2007; ~0.505 Pg, CCSP 2007) remains unknown. Forest carbon storage accounting projects are of significant interest to many international organizations (e.g., United Nations Framework Convention on Climate Change (UNFCCC, 2015), the Intergovernmental Panel on Climate Change (IPCC) (Nabuurs et al., 2007) and Food and Agriculture Organization of the United Nations (FAO) (Forestry department, 2015)), federal governments (e.g., Brazil, (Sills et al., 2014, pp. 51-143); Indonesia, (Sills et al., 2014, pp. 290-397) ; Norway, (Bartlett et al., 2020); Australia, (Australian Government, 2018); Canada (Kurz & Apps, 2006); United States (U.S. Forest Service, 2023)) and more recently, municipalities and cities (e.g., "Urban Forest Strategy" implemented in Melbourne, Australia, (City of Melbourne, 2012); and "Urban Forest Action Plan" in City of Portland, Oregon, United States, (PPR 2020)).

Before the contemporary focus on forest carbon storage and sequestration due to their ability to mitigate fossil-fuel combustion and regulating climate change (Canadell & Raupach, 2008), trees and the estimation of their biomass played a crucial role in timber production. Originally, biomass estimates were focused on tree stem volume since only the stem could be used for merchantable wood (Carpenter, 1985). Early historical approaches to estimate tree biomass and volume included taper equations (e.g., Hojer taper Model (Hojer, 1903), Ormerod taper model (Ormerod, 1973)), volume (weight) tables (e.g. Spurr, 1952; Chaturvedi and Khanna, 1994), and allometric equations (Carpenter, 1985). Later, in the 1950s, destructive sampling was used to establish a statistical relationship between a simple measurement that could be conducted with ease in the field by a forester (i.e., diameter at breast height (DBH) often acquired at 1.37m above ground) with tree biomass, which was determined by cutting and weighing the aboveground woody components (Catchpole & Wheeler, 1992). The generation of allometric equations has proven incredibly useful in the estimation of biomass and carbon for decades (Ruark et al., 1987), especially when the

equations are derived and used locally as they yield higher accuracy than generic-multi-species equations or from same species located geographically distant from where they are applied (Kim et al., 2011, Van Breugel et al., 2011). Regardless of their origin, the individual-tree application of allometriequations has not been scalable to large spatial extents due to the time requirements to conduct tree inventories (Vorster et al., 2020), which include manual DBH measurements and tree species identification.

Efforts to scale allometric equations to larger spatial extents has been done by aggregating individual tree estimates to a sampling area or plot to derive an estimate of biomass density (e.g., kg / ha) that is multiplied against the larger area of a particular forest, forest stand, or some other areal definition of tree cover (e.g., Ravindranath & Ostwald, (2008)). The contemporary equivalent to this approach is referred to as an inventory or benefits transfer approach, whereby in-situ estimates of biomass and carbon are summarized and applied to digital maps generated from remotely sensed data (e.g., Robinson et al. 2023; Chave et al., 2019). While this approach has advanced our ability to quantify and map biomass and carbon across large spatial extents, the approach does not capture spatial variability in individual tree biomass due to site and situation conditions and is likely to contain substantial error (Vorster et al., 2020).

In an effort to improve forest and tree biomass estimates, terrestrial laser scanning has been conducted using Light Detection and Ranging (LiDAR) sensors (e.g., Raumonen et al., 2015; Liang et al., 2016; Disney et al., 2018). The ground-based approach is able to generate a very-high resolution point cloud (e.g., ±2mm at 25m, (Kankare et al., 2013)) that can be used to measure tree characteristics such as tree height, DBH and crown width (Srinivasan et al., 2015). Added value is gained by segmenting individual-tree point clouds and using them as input to one of various methods that can create a three-dimensional (3D) reconstruction of the tree, such as Quantitative Structural Modelling (QSM) (Brede et al., 2022; Calders et al., 2015; de Tanago et al., 2018; Raumonen et al., 2015) and voxelization (Hosoi et al., 2013). The volume of the 3D reconstructed tree multiplied by the tree's wood density yields an estimate of tree biomass, which is conceptually equivalent to destructive sampling. The challenge from the use of the terrestrial laser scanning is that results are spatially constrained, it can be difficult to acquire accurate global navigation satellite system receiver readings in dense canopy forests (Yoshimura & Suzuki, 2019) and the time required to triangulate and calibrate the scanner for a relatively small area (e.g., 0.1 ha) can be substantial (Jaafar et al., 2018).

Airborne or satellite-based remote sensing are approaches used to overcome the spatial constraints of in-situ tree inventory measurements and terrestrial laser scanning. While spatial resolutions from satellites continue to become finer (e.g., Pleiades, 0.50 m, Perko et al., 2018), and space-borne LiDAR such as GEDI and ICESat-2 (Liu et al., 2021) offer the ability to generate canopy height models (e.g., GEDI 25m footprint), there remain accuracy issues (Kaartinen et al., 2012), which are particularly relevant if biomass and carbon estimates are to be used for local management and decision-making. Furthermore, optical data from space may have high resolution but still incur quality issues due to atmospheric effects (e.g., Bansod et al., 2017) and LiDAR data from space as well as mid-altitude aircraft are too sparce for use in 3D tree reconstruction. For

example, GEDI produces point cloud densities at around 35 pts/$m^2$ (Liu & Wang, 2022), recent LiDAR mid-altitude piloted aircraft in Ontario, Canada, collects at densities ranging from 8-27 pts/$m^2$.

A bridge between in-situ and large-scale remote sensing capabilities is provided by Remotely Piloted Aircraft (RPA). Not only can RPA flight parameters be manipulated (e.g., low and slow) to generate very high-resolution imagery (<0.02m) and very dense point clouds (>300 pts/$m^2$) with minimal atmospheric affects, but their on-demand deployment enables data to be collected coincidentally with in-situ measurements. The high-resolution imagery and high-density point-cloud data acquisition from RPA can be used for 3D reconstruction of individual trees, which can improve the accuracy of forest and individual tree biomass and carbon estimates as well as foster the generation of novel allometric equations. To improve our understanding about how RPA data can be used to estimate biomass and carbon, we sought to determine: 1) what was the accuracy between RPA acquired LiDAR data and in-situ measurements of diameter at breast height? 2) In addition to question 1), we also asked what was the degree of correspondence between in-situ estimates of biomass and carbon compared to those derived using RPA acquired LiDAR data? To answer the first question, we used two Quantitative Structural Models (QSMs) to 3D tree reconstruction and compared those reconstructions to in-situ measurements. To answer the second question, we compare estimated biomass and carbon from our QSM results to those generated from a compilation of allometric equations harvested from the literature and i-Tree Eco. In both comparisons we assess the effects of using point cloud data collected during leaf-on versus leaf-off conditions, tree size via DBH class, and a low tree-density forest site versus a high tree density forest site. Lastly, to ensure replicable results and useable methodology for others, we follow the findable, accessible, interoperable, and reusable (FAIR) principles for code development and make all data and code freely available online.

# 2 Method

## 2.1 Study site

Our study resides within the Hullett Provincial Wildlife Area (HPWA) located in Southwestern Ontario, Canada (Fig. 1). The HPWA is a 2200-hectare property owned by the province of Ontario and managed in partnership with the Ministry of Natural Resources and Forestry, Ducks Unlimited Canada, and the not-for-profit group Friends of Hullett. The overarching goal for the property, as outlined in the 1985 Management Plan, is to “manage its resources to provide opportunities for high quality, wildlife-based day-use recreation experiences for the people of Ontario” (OMNR 1985, pg. 4). One of the objectives within the Management Plan involves managing forests within the area for the production of wood products, when consistent with the overarching goal.

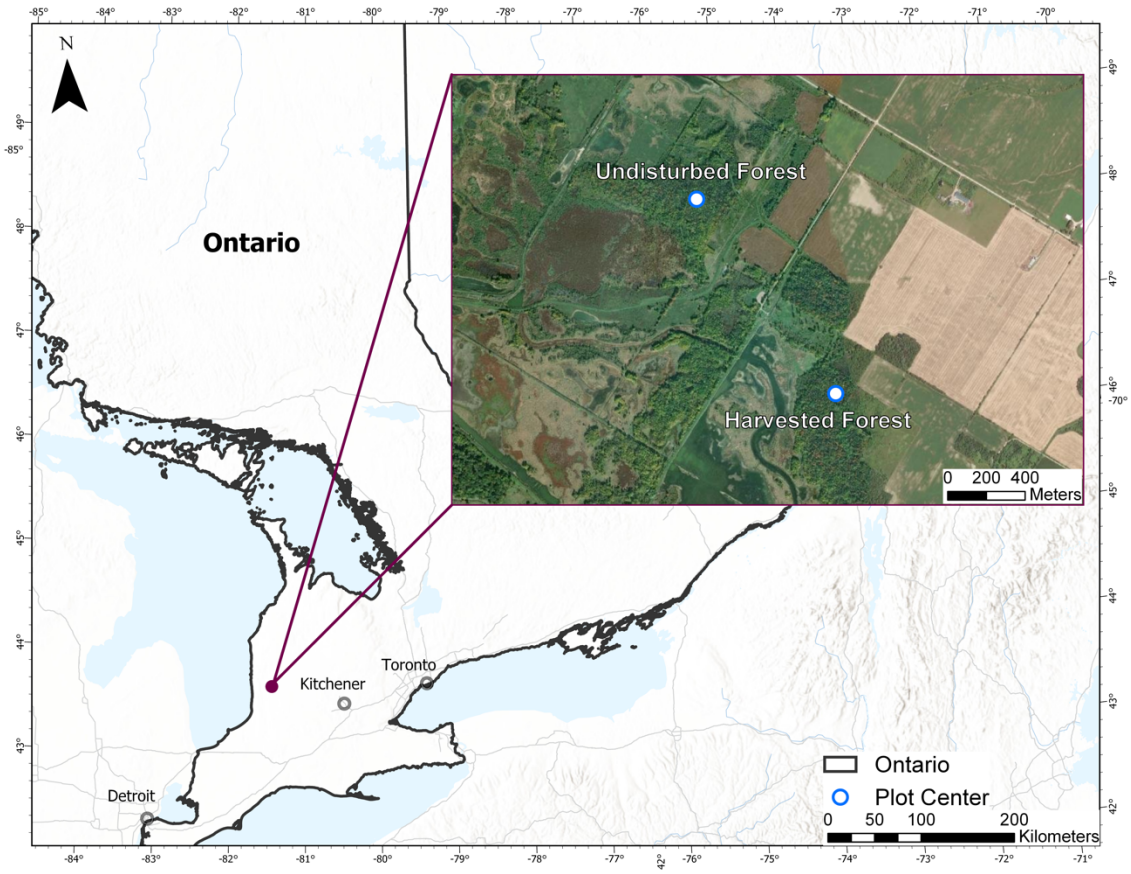



*Figure 1. Study area within Hullett Wildlife Preserve, southwestern, Ontario, Canada. The study area consisted of two forest plots that were located in core forest area. One plot was a younger plot with higher tree density that had been undisturbed (Undisturbed). The other plot was an older forest that had been selectively harvested and had a lower tree density (Harvested).*

In 2008 a Habitat Management Plan was approved to provide details on how specific habitats will be managed to meet the goal and objectives of the Management Plan. The goal of the Habitat Management Plan is to "manage the land resources of the Hullett Provincial Wildlife Area to provide a diversity of high-quality wildlife habitat" (OMNR 2008, pg. 8). Among six principles, the Habitat Management Plan specifies the following specifically for forests: upland woodlots will be managed to provide wildlife habitat, timber harvests and aesthetic values to users; healthy ecosystems require a minimum of 30% forest cover, and at a landscape level, at least one forest patch of 200 ha, with a minimum width of 500 metres; Native species will be favoured in management programs; economic returns from agricultural land rental, and forest products are acceptable as long as they don't have significant negative impacts on other management objectives."

In 2018 a harvesting prescription for tree salvage was written by GWG Resources Services and trees were marked again. Selective logging was completed over the winter of 2021/2022. The ecologist with the MVCA was hired to conduct establish two Vegetation Sampling Protocol plots to quantify the condition of the HPWA woodlots. One was established in woodlot that was

harvested in January/February 2022 (Harvested) while the other was established in a woodlot that hadn't been disturbed in decades and is remote (Undisturbed). The Harvested site comprised 30 trees, which were dominated by Green Ash (40%), Sugar Maple (30%), American Elm (17%). Other species were American Basswood (10%), Eastern Hophornbeam (3%). The Undisturbed site comprised 63 trees, which were dominated by Sugar Maple (44%), Green Ash (29%), American Elm (16%). Other species present were American Basswood (3%), Eastern Hophornbeam (3%), White Ash (3%). The plots are meant to provide a baseline of forest conditions and validate some of the observations and opinions.

### 2.2 In-situ sampling

Our in-situ measurements took place in two plots that were selected to compare different forest conditions (Harvested, and Undisturbed). In each plot, a vegetation sampling protocol (Puric-Mladenovic and Kenney, 2015) was conducted on August 29, 2023, to record general plot descriptive characteristics, vegetation class, surface topography, tree height, diameter at breast height (DBH) and crown health, down woody debris, regeneration, disturbance and soil characteristics. Only a portion of the protocol specific to the acquisition of our tree cover data is described herein.

Unlike a timber cruise method (Girard and Gevorkiantz, 1939) the implemented protocol uses a fixed-area sampling method to ensure measurements could be replicated and tracked over time. The fixed location allowed for the acquisition of Remotely Piloted Aircraft data during leaf-on and leaf-off conditions as well as permits the plots to be revisited in the future. For each of our two fixed-area plots, the centre was a tactical selection based on approximating our random point selection using a global navigation satellite system receiver. Plots were circular in shape, with a radius of 11.28 m, creating a total plot area of 400 $m^2$. Lines were stretched in the four cardinal directions (North, East, South, West) to facilitate measuring in sections and subplots related to ground cover were established along these lines. The protocol excludes trees less than 5 cm DBH and down woody debris less than 7.5 cm in diameter.

Each tree within a plot received a unique identifier number and was measured for DBH at approximately 1.37 m above ground level (West, 2015). If multiple stems were present at that height, then each stem DBH was recorded. The species of each tree was recorded and the height of several trees within each plot were estimated using a clinometer. If a tree was dead, it was labelled as a snag. If a tree was dead an presented a hazard it was labelled as a hazard. These types of labels are useful for aligning remotely sensed data with the in-situ measurements. The geographic location of each tree within the two plots was determined to ensure an accurate alignment between RPA data collection and in-situ measurements. To achieve location accuracy within the two forest plots, a Leica GS18 Global Navigation Satellite System Receiver, with accesses to multiple satellite constellations (i.e., Global Positioning System, US; Galileo, Europe; BeiDou, China) and a real-time kinematic correction service (i.e.,HxGN SmartNet) operationalized over the cellular network enabled the acquisition of an average point location

accuracy for trees in the Harvested plot (n = 30) of 0.053 m in the horizontal direction, 0.073 m in the vertical direction, and an average 3D accuracy of 0.091. The accuracies for the undisturbed plot (n = 63) were 0.504 m in the horizontal direction, 0.874 m in the vertical direction, and an average 3D accuracy of 1.014 m. The average horizontal and vertical error across both plots was 0.360 m and 0.618 m, respectively, with an average 3D error of 0.720 m.

### 2.3 Remotely Piloted Aircraft sampling

Remotely sensed data were collected twice, once during the leaf-on period (August 31, 2024) when the canopy was dense and once during the leaf-off period (December 6, 2024) prior to snow fall. A DJI Matrice 600 Remotely Piloted Aircraft with an integrated Riegel MiniVUX-1 light detection and ranging (LiDAR) sensor and 24 MP Sony A6000 camera was used for data collection. The MiniVux-1 has a 360-degree field of view and was configured to operate with a measurement rate of 100,000 measurements per second at 100 kHz pulse repetition rate. The laser beam divergence is 1.6 x 0.5 m rad, which generates a laser beam footprint of 160 mm x 50 mm at 100 m altitude above ground. The aircraft was flown at 60m above ground level (flight speed of 3 m/s) with LiDAR scan lines 0.1 m apart and only points within a 120° field of view were retained to acquire point densities approximating 300 pts/$m^2$ within our study area (average of 193 pts/$m^2$ for each flight line). The footprint diameter was 0.0273 m on average with a minimum of 0.0212 m and maximum of 0.0424 m.

Three flights were flown with the first two generating perpendicular flight patterns, commonly referred to as a grid pattern, and a third flight flown with the flight lines running at a 45-degree angle to the previous two flights (i.e., flight 1 east-to-west, flight 2 north-to-south, flight 3 northeast-to-southwest). The combination of all three flights yielded a point cloud density > 900 pts/$m^2$. The optical imagery was acquired with 75% sidelap and 80% forward overlap among images with a ground sampling distance of 0.01-0.02 m. The remotely sensed data were used to measure the following tree characteristics to coincide with in-situ measurements: crown width and area, tree height, diameter at breast height (DBH), tree count, and the classification of over or understory. The remotely-piloted-aircraft-acquired DBH measurement is compared against the in-situ measurements and used with allometric equations (Section 2.4.1) to estimate aboveground tree biomass and carbon. The full point cloud acquired by the Remotely Piloted Aircraft is used in the virtual 3D reconstruction of individual trees (Section 2.4.2) to estimate their biomass and carbon.

### 2.4 Biomass estimation methods

Traditional methods of estimating tree biomass, like destructive sampling or manually measuring tree dimensions can damage trees and the ecosystems within which they reside and can be labor-intensive (Disney et al., 2018). The application of LiDAR technology offers a non-destructive approach to tree measurement by capturing intricate three-dimensional details of trees and forests (Hosoi et al., 2013). This technology, particularly through Terrestrial Laser Scanning (TLS) (Calders et al., 2015; Kankare et al., 2013; Lau et al., 2018; Raumonen et al., 2013) and Remotely Piloted Aircraft System (Brede et al., 2019; ), enables the measurement of tree attributes such as

tree height, area, and branch architecture, which are used in the estimation of aboveground tree biomass. An indirect estimation of aboveground tree biomass can be achieved using Allometric Scaling Models, which capture relationships between tree parameters (e.g., DBH) and biomass in what is known as an allometric equation (e.g., West et al., 1999) or by using three-dimensional (3D) reconstruction techniques such as Quantitative Structural Modelling (QSM), which involves segmenting a tree into separate sections and approximating each segment with a regular-shaped geometry. By calculating the volume of each segment and obtaining the accumulative volume, the biomass of trees can be acquired with the combination of the wood density.

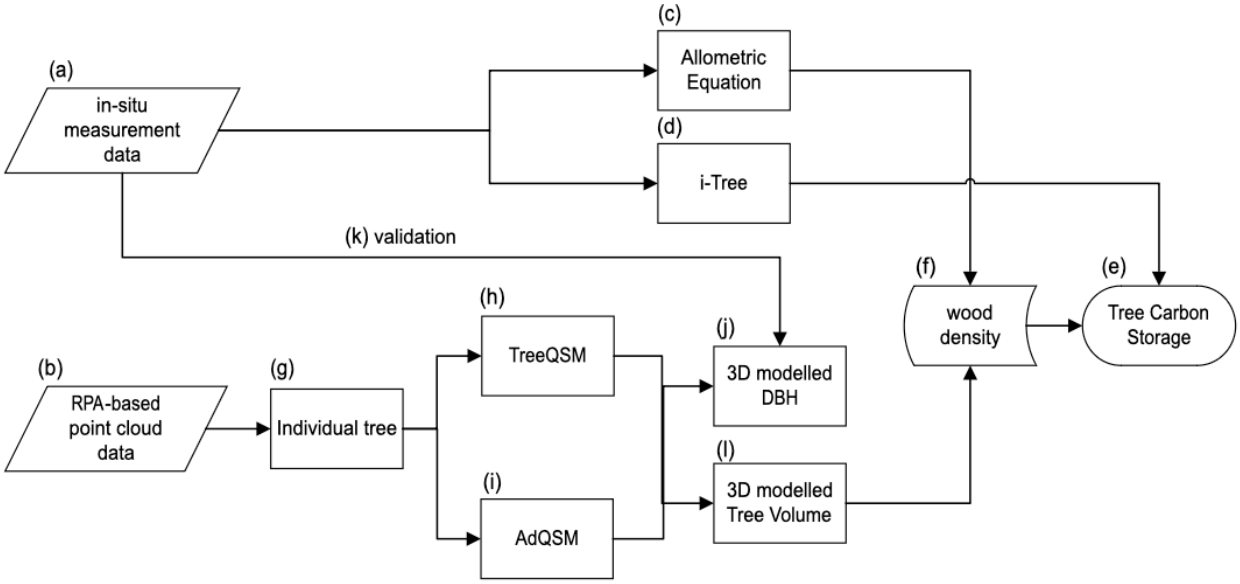



*Figure 2. Methodology for comparative analysis of tree carbon estimates from allometric and Quantitative Structural Modelling (QSM) approaches. Parallelograms (a, b) represent data inputs; Rectangles (c, d, g, h, i, j, l) indicate processes or operations; Pentag (f) denotes external data; Oval (e) signifies the final output.*

To evaluate the accuracy of RPA acquired LiDAR and subsequently compare estimates of biomass and carbon from allometric and 3D reconstruction approaches, our methodology first involved collecting both in-situ data and RPA-based point cloud data on the same day (Fig. 2 (a, b)). The in-situ data were used as input to the two Allometric Scaling Models (ASMs) (Fig. 2 (c, d)). The i-Tree Eco model outputs tree carbon values directly (Fig. 2e), whereas some allometric equations obtained from the literature estimate volume and require wood density values (Fig. 2f) to estimate tree biomass and carbon. Paralleling the ASMs, the QSM approach involved manually segmenting the RPA-based point cloud data (Fig. 2b) to derive point cloud data for individual trees (Fig. 2g). The point cloud data for individual trees were input into the quantitative structural models TreeQSM (Fig. 2h) and AdQSM (Fig. 2i). The quantitative structure models derived estimates DBH (Fig. 2j) that were compared against in-situ measurements to assess or validate their performance (Fig. 2k). The two QSMs also estimated tree volume (Fig. 2l), which like some allometric equation volume estimates, were multiplied by wood density to derive individual tree-biomass estimates. While conversion of biomass to carbon can vary between 0.48-0.53 depending

on species, tree component, and other factors (e.g., Gower 2003), we used a biomass to carbon coefficient of 0.5, which is most frequently used in the literature and facilitates comparative analyses with others (e.g., Brown and Lugo, 1982; Chow and Rolfe, 1989; Keith et al., 2009; Roxburgh et al., 2006, West, 2015).

*2.4.1 Allometric Scaling Model*

Allometric Scaling Models (ASMs) are typically developed by relating destructive tree sampling biomass measurements to easily measurable tree characteristics (e.g., diameter at breast height, tree height). Unlike a single allometric equation, ASMs often refer to a collection of multiple allometric equations, and some models also account for the effects of human-induced or natural disturbances on biomass. Since this study does not focus on the selection or analysis of individual allometric equation, both approaches are collectively referred to as ASMs in the following sections. Commonly used ASMs incorporate one or more dependent variables and are most differentiated by those using only DBH, and those using both DBH and tree height. The inclusion of tree height typically increases biomass estimation accuracy (Yang et al., 2022); however, tree height measurements are difficult to obtain with accuracy in forest stands and add additional challenges during destructive sampling, which is partly why there are fewer allometric equations that incorporate height.

The basic form of typical allometric equation is a simple power function:

$$B = a \times DBH^{b} \tag{2}$$

Where $B$ is biomass (kg), $DBH$ is the diameter at breast height (1.37m) in cm, and parameters $a$ and $b$ are statistically determined. The allometric equation can be linearized using a logarithmic transformation:

$$\ln(B) = \ln(a) + b \times \ln(DBH) + \varepsilon \tag{3}$$

When data are transformed to a logarithmic scale, the residual errors ($\varepsilon$) are presumed to follow a normal distribution with an average of zero and a uniform variance. When tree height data are accessible, the allometric equation takes the following form with parameters $c$ also statistically determined from the destructive sample:

$$B = a \times DBH^{b} \times H^{c} \tag{4}$$

ASMs are normally developed through a comprehensive process of destructive sampling (Picard et al., 2012), and substantial effort has gone into refinement of allometric equations for specific species and regional applications, acknowledging that a large sample size is needed to derive robust equations (Yang et al., 2022). However, destructive sampling is a labor-intensive and costly data acquisition (Disney et al., 2018). Non-destructive sampling methods involving LiDAR offer a cost and time effective alternative to destructive sampling with minimum-to-no impact on the

ecosystem that can yield substantially larger sample sizes and can contribute to the creation of regionally specific allometric equations. Historically, terrestrial laser scanning (TLS) has been used as a non-destructive sampling approach to estimate biomass and generate local allometric equations (e.g., Aguilar et al., 2019; Lau et al., 2019; Stovall et al., 2018, 2023). The increased regional specificity typically yields more accurate biomass estimates than national equations Case and Hall (2008) and species-specific equations also increase accuracy relative to general-species equations Annighöfer et al. (2016). Additionally, Roxburgh et al. (2015) explored the relationship between sample size and model accuracy and demonstrated that larger sample sizes improve the model's capacity for generalization.

Although the pathways to more accurate allometric growth models are known, numerous challenges persist. For instance, ASMs are often derived from empirical measurements taken within specific locales or from trees of certain size classes, which limits their broader application (Disney et al., 2018). Even within the same species, the disparity between results from small-scale local equations and national equations can be substantial. As noted by Xing et al. (2019), inaccuracies can escalate, leading to as much as a 12% overestimation of stand-level aboveground biomass, contingent upon forest cover type. Moreover, databases typically offer a limited selection of species-specified allometric models for local tree varieties, because destructive sampling often targets standard growth dominant trees, this results in less accurate estimates for trees at the extremes of diameter classes—smaller and larger trees—which are less frequently sampled. Despite allometric growth models being the most widely utilized method for estimating the aboveground biomass of trees, there are still many unresolved issues associated with their use.

In this study, we employed two ASM tools. First, we conducted an extensive literature search to harvest allometric equations and integrate them into a Jupyter Notebook using the R 4.2.0 kernel that is open source. We acquired 1,058 formulas representing all or parts of 285 different tree species and estimated tree carbon for each tree in our sample sites using this tool. The tool has much broader utility and has been run successfully with up to 150,000. Then, i-Tree Eco (hereinafter referred to as i-Tree) (https://www.itreetools.org/tools/i-tree-eco) developed by the US Forest Service was used to estimate individual tree carbon. The i-Tree model uses a variety of tree characteristic (e.g., species, DBH, height, crown health), land use (e.g., residential, park, wetland) and status (e.g., planted, ingrowth) inputs to generate estimates of carbon storage, carbon sequestration, and other ecological functions (e.g., precipitation interception). The minimum requirements for running i-Tree are tree species and DBH measurements. While i-Tree is open access and freely available for use, our team is interested in knowing, which specific equations are used and we, like many, are trying to ensure our research is findable, accessible, interoperable, and replicable (i.e., FAIR compliant, Wilkinson et al. 2016).

*2.4.2 Three-Dimensional (3D) Reconstruction*

Each tree has a distinct spatial structure that is the outcome of myriad factors affecting tree growth (e.g., competition for light and nutrients, soil characteristics and water holding capacity, slope and

topology), and this uniqueness persists even among trees of the same species growing under similar environmental conditions. In this context, 3D reconstruction is emerging as a critical approach to derive detailed models of single trees or their collection in forest areas to support precise, quick, and automated modeling of tree structures and their geometric properties. The techniques for 3D reconstruction currently employed in research can generally be classified into three categories: 1) Voxel-derived volume methods (Hosoi et al., 2013; McHale, 2008), which rely on voxel-based volumetric analysis; 2) Point structure estimation techniques (Kankare et al., 2013; Srinivasan et al., 2014), focusing on estimating structures from point data and stem curve; and 3) Quantitative Structure Modeling (QSM) (Calders et al., 2015; de Tanago et al., 2018; Disney et al., 2018; Thies et al., 2004), which is a method for creating detailed structural models of trees. In the following sections, we delve into the foundational principles and practical applications of the Quantitative Structural Modeling.

An approach to 3D tree reconstruction that originated nearly two decades ago (e.g., Raumonen et al., 2013), is known as Quantitative Structural Modelling (QSM, Disney et al., 2018). The modelling approach can be conceptualized as comprising six steps: obtaining a point cloud of a tree, segmenting that point cloud into sections of the stem and branches, fitting cylinders to the points in each segment (e.g., Hackenberg et al., 2014), calculating the volume of the cylinder, and finally, summing up the cumulative volume of all generated cylinders. How each of these steps are operationalized and visualized differentiates one QSM approach from another (e.g., AdQSM, Fan et al. (2020); TreeQSM, Raumonen et al., (2013); SimpleTree, Hackenberg et al., (2015); PypeTree, Delagrange et al., (2014)). The estimation of tree biomass and carbon from the QSM approach is a final simple step that involves multiplying the estimated tree volume by the wood density of the tree to obtain an estimate of biomass and dividing that biomass in half to derive an estimate of carbon.

Validation of QSM approaches have taken different forms. For example, a virtually constructed artificial tree was used in combination with Monte Carlo simulated Terrestrial Laser Scanning (TLS) point clouds to quantify that an error margin of 5–10%, was attainable using a QSM approach (Raumonen et al. 2013). In another case, TLS scanning and QSM were compared to destructive harvest measurements of 20 tropical trees, yielding a concordance correlation coefficient of 0.95 and evidence that results were not affected by tree structural characteristics (de Tanago et al. 2018). Another tropical destructive sampling study, comprising 26 trees, found QSM derived tree characteristics were very similar to field measurements, e.g., observed vs QSM diameter at breast height were 16.7-128.7, 16.7-130.2 cm, respectively (Lau et al. 2018). Often the overarching goal of data collection and modelling is to generate localized allometric equations, which in this case led to TLS QSM derived allometric equations yielding $R^2$ 0.92-0.93 with field biomass measurements.

Similar to the use of TLS data with QSM based approaches for tree biomass estimation, Remotely Piloted Aircraft LiDAR scanning (RPA-LS) has also been used. When compared to TLS-QSM,

one study of mature beech and oak stands achieved a Concordance Correlation Coefficient (CCC) of 0.85, with a decrease in performance with smaller branches and denser stands. The flexibility of QSM for TLS and RPA applications offers a leap forward in the non-destructive evaluation of tree biomass, paving the way for improved allometric models and enhanced precision in biomass and carbon emission assessments.

Among the three 3D reconstruction approaches mentioned above, QSMs stand out as the most precise method for assessing tree volume, aboveground biomass, and architecture (Disney et al., 2018). However, this method is not without its uncertainties. Factors such as inherent variations in the reconstruction procedures, trunk shapes, and the presence of needles and leaves can influence the quality of the 3D reconstruction (Disney et al., 2018; Ye et al., 2019). Nevertheless, no study has yet validated this claim by directly comparing these methods. Given this context, the primary goal of our research is to fill this knowledge gap. To do so, we compare TreeQSM and AdQSM in their ability with LiDAR data to replicate in-situ DBH measurements and compare their estimation of biomass and carbon relative to estimates acquired using allometric equations obtained from literature and those derived from i-Tree. Through this comparative effort, we hope to offer definitive insights into the relative accuracy and robustness of QSMs compared to other prevalent tree estimation techniques as well as provide a benchmark for others to compare their work.

TreeQSM (Raumonen et al., (2013), https://github.com/InverseTampere/TreeQSM) is an advanced software tool developed in MATLAB, specifically designed for constructing QSMs from tree point cloud data collected via terrestrial laser scanning. This software excels in providing detailed assessments of tree structural metrics such as trunk volume, branch volume, number of branches, DBH, tree height. The core of TreeQSM's model reconstruction lies in the appropriate setting of three critical parameters: PatchDiam1, PatchDiam2min, and PatchDiam2Max. These adjustable patch diameters are strategically placed on the tree to outline its overall structure. Different patch diameters serve distinct functions: initially, the algorithm uses a uniform and larger PatchDiam1 to filter irrelevant points. Subsequently, to differentiate between the trunk and branches, patches of varying sizes are employed, ranging from the smaller PatchDiam2min to the larger PatchDiam2max. The use of variable-sized patches allows TreeQSM to delineate and quantify components of a tree's complex branching patterns.

AdQSM (Fan et al. (2020)) is a C++ developed 3D tree model reconstruction method based on terrestrial laser scanning point clouds. Building upon (AdTree, Shenglan Du et al. 2019), which offered high modeling precision and visualization of 3D tree reconstruction. AdQSM incorporated tree metrics and validation. against the destructive sampling of 29 tropical trees. Results of these validation efforts yielded an $R^2$ of 0.94 between modelled and observed DBH, and $R^2$ of 0.96 between modelled and observed volume. AdQSM utilizes two essential parameters: height segmentation (HS) and cloud parameter (CP). HS determines the height of each segment in the point cloud data, while CP determines the extraction rate of the point cloud. According to the software's instructions, CP is recommended to remain fixed, HS should be adjusted to produce

different outcomes. The average of these reasonable outcomes is then taken as the representative value for the tree.

*2.4.3 QSM Calibration*

The calibration of the two Quantitative Structure Models, TreeQSM and AdQSM, took slightly different approaches. TreeQSM contains three parameters requiring specification for a model run: PatchDiam1, PatchDiam2Min, PatchDiam2Max. TreeQSM partitions an input point-cloud data into patches (i.e., groups of points) and each of the PatchDiam parameters affect how the creation of patches occurs. The first parameter, PatchDiam1 (length in m), is used to filter out irrelevant points (e.g., noise) and create an initial set of point-cloud partitions. These initial partitions are uniform in length and larger than subsequent partitions. Using these initial partitions, subsequent patches are created that vary in size and range from smaller PatchDiam2Min to PatchDiam2Max, whereby Min represents the tips of branches and Max represents the size at the base of the tree stem (in m). Specifics of the model and parameterization are discussed elsewhere (Raumonen et al. 2013, and TreesQSM Version 2.4.1 Manual).

To calibrate TreeQSM, our tree sample data were subset (70%) for model training. Calibration proceeded through an iterative process that involved modifying parameter values for PatchDiam1, PatchDiam2Min, and PatchDiam2Max, as well as the number of models run. The standard calibration approach for TreeQSM involves systematically sweeping parameters at regular intervals (Raumonen, 2022), but this approach often limits the parameter space explored. Instead, we sought to explore a broader parameter space and used a Monte Carlo approach, which randomly selected parameter values within predefined ranges for the three PatchDiam parameters (PatchDiam1 0.05-0.10, PatchDiam2Min 0.02-0.06, and PatchDiam2Max 0.03-0.15). TreeQSM contains stochasticity in its model generation, therefore each tree was modeled 25 times (5 iterations with 5 model runs per iteration). To assess model accuracy, the DBH for each modelled tree in the training set was calculated and compared to the observed in-situ DBH using the Root Mean Square Error (RMSE). The parameter configuration that yielded the lowest RMSE during the training phase was then used in our validation assessment (i.e., testing phase).

The calibration of AdQSM was much simpler as there are only two free parameters to manipulate. The first is known as the height segmentation (HS) parameter. It controls the height of each partition of the point cloud and therefore the number of segments. We systematically increased the HS parameter at increments of 0.05 from 0.4 to 1.0 to generate 30 models for each tree. The second parameter, the cloud parameter, specifies the maximum number of points in the cloud that are used in the cylinder fitting process in each segment specified by the HS parameter. The cloud parameter was kept at the default value of 0.003 as suggested in the software's instructions. The final AdQSM-estimated DBH was obtained by averaging the outcomes after excluding extreme values to ensure accuracy. The final AdQSM-estimated DBH was calculated by averaging the results after excluding extreme values. These extreme values were identified when certain HS parameters produced results with significant deviations from others using the same tree point cloud data, or

when the model visualization exhibited substantial discrepancies or failed to generate a successful model. In such cases, these outliers were excluded to ensure the accuracy of the average DBH.

# 3 Results

## 3.1 QSM Validation

### *3.1.1 Leaf on versus Leaf off*

The distribution of DBH values from all in-situ measurements (i.e., both sites combined) had a mean 15.98 cm and standard deviation of 9.57 cm among our sample of 93 trees in leaf-on season (August 31, 2023; Table 4). When pooled together, we obtained contrasting outcomes from the two QSM approaches. TreeQSM yielded an average DBH (39.14 cm) that was 23cm more than in-situ DBH average. However, the standard deviation was more than 5 times greater (55.18 cm) than the distribution of in-situ DBH measurements. A Pearson Correlation of in-situ and TreeQSM DBH values ($r = 0.05$) showed little correspondence despite the similar mean score. While AdQSM provides a more aesthetically pleasing visual output as well as simpler operation than TreeQSM, it also yielded better results overall. The distribution of DBH values estimated by AdQSM had a similar spread to the in-situ measurements (sd = 7.40 cm), but the mean DBH was much higher (27.77 cm), which exhibited less overlap with our in-situ measurements compared to TreeQSM. A Pearson Correlation of in-situ and AdQSM DBH values was moderate correlation ($r = 0.57$), suggesting more alignment and consistency with in-situ measurements than TreeQSM. The calculation of error metrics reinforced these findings, such that TreeQSM had greater error and less fit (RMSE = 58.37, MAE = 32.27, $R^2 = 0.002$) than AdQSM (RMSE = 8.51, MAE = 6.03, $R^2 = 0.33$).

During the leaf-off season (December 6, 2023), the distribution of DBH values from all in-situ measurements had a mean 15.27 cm and a standard deviation of 8.97 cm among our 86-tree sample (Table 4). Tree mortality consumed seven trees between the two data collection dates. With the leaf-off data. we again received different outcomes from the two QSM approaches (Fig. 3). The mean TreeQSM DBH (12.45 cm) underestimated the in-situ value of 15.27 cm, which was a greater difference than obtained during the leaf-on season. However, in the leaf-off season, the standard deviation of DBH obtained by TreeQSM (5.86 cm) was much closer to the in-situ value. The correspondence between the TreeQSM DBH values and the in-situ values was worse and in the opposite direction as demonstrated by a Pearson Correlation of -0.12. Using the leaf-off data, the performance of AdQSM improved. Despite overestimating the distribution of DBH scores relative to the in-situ measurements (mean = 23.41 cm, sd = 7.05 cm), the Pearson Correlation was high ($r = 0.81$). Error metrics also demonstrated that TreeQSM (RMSE = 11.64, MAE = 8.77, $R^2 = 0.02$) had greater error and did not fit the data as well as AdQSM (RMSE = 9.57, MAE = 8.22, $R^2 = 0.66$) using our leaf-off data.

*Table 4. Summary of in-situ and DBH estimation (cm) and accuracy results for TreeQSM and AdQSM in Harvested and Undisturbed forest sites during leaf-on and leaf-off seasons. sd = standard deviation, RMSE = root mean squared error, MAE = mean absolute error, MAPE = mean absolute percentage error.*

| | | In-Situ | | TreeQSM | | AdQSM | |
|---|---|---|---|---|---|---|---|
| | | Leaf On | Leaf Off | Leaf On | Leaf Off | Leaf On | Leaf Off |
| **All Trees** | Tree Count | 93 | 86 | 56 | 85 | 30 | 79 |
| | Mean | 15.98 | 15.27 | 39.14 | 12.45 | 27.77 | 23.41 |
| | sd | 9.57 | 8.97 | 55.18 | 5.86 | 7.40 | 7.05 |
| | r | - | - | 0.05 | -0.12 | 0.57 | 0.81 |
| | RMSE | - | - | 58.37 | 11.64 | 8.51 | 9.57 |
| | MAE | - | - | 32.27 | 8.77 | 6.03 | 8.22 |
| | MAPE | - | - | 212.02 | 64.49 | 30.95 | 87.11 |
| | $R^2$ | - | - | 0.00 | 0.02 | 0.33 | 0.66 |
| **Harvested** | Tree Count | 30 | 26 | 27 | 26 | 16 | 26 |
| | Mean | 19.92 | 17.92 | 29.97 | 12.56 | 28.30 | 25.99 |
| | sd | 11.97 | 11.36 | 32.02 | 5.91 | 5.82 | 6.87 |
| | r | - | - | -0.32 | -0.37 | 0.76 | 0.97 |
| | RMSE | - | - | 37.60 | 14.47 | 5.59 | 9.29 |
| | MAE | - | - | 26.70 | 11.43 | 3.91 | 8.17 |
| | MAPE | - | - | 225.61 | 77.21 | 17.59 | 90.60 |
| | $R^2$ | - | - | 0.10 | 0.12 | 0.57 | 0.83 |
| **Undisturbed** | Tree Count | 63 | 60 | 29 | 59 | 14 | 53 |
| | Mean | 14.10 | 14.12 | 47.67 | 12.40 | 27.16 | 22.41 |
| | sd | 7.60 | 7.54 | 69.81 | 5.89 | 9.07 | 6.92 |
| | r | - | - | 0.28 | 0.03 | 0.62 | 0.74 |
| | RMSE | - | - | 72.54 | 9.75 | 10.93 | 9.70 |
| | MAE | - | - | 37.46 | 7.32 | 8.45 | 8.24 |
| | MAPE | - | - | 199.36 | 57.56 | 46.22 | 85.40 |
| | $R^2$ | - | - | 0.08 | 0.00 | 0.38 | 0.56 |

Comparison of leaf-on versus leaf-off for both TreeQSM and AdQSM demonstrated that leaf-off data yielded better results and that TreeQSM consistently performed poorly relative to AdQSM. Reduced error and better model fit using leaf-off data can be attributed to reduced leaf occlusion, which enabled the point cloud to best represent the stem and branches (i.e., the woody biomass) of our sample trees and subsequently improved the cylinder fitting algorithms of the QSM approaches. These results, from pooling all trees, demonstrate that AdQSM is able to derive a moderate fit to in-situ DBH measurements with an average DBH error between 6.03 cm and 8.22 cm. Qualitative in-field comparisons have shown DBH measurements can vary by +/- 2.00 cm, which suggests that opportunity exists for the QSM approach with further refinement and error reduction.

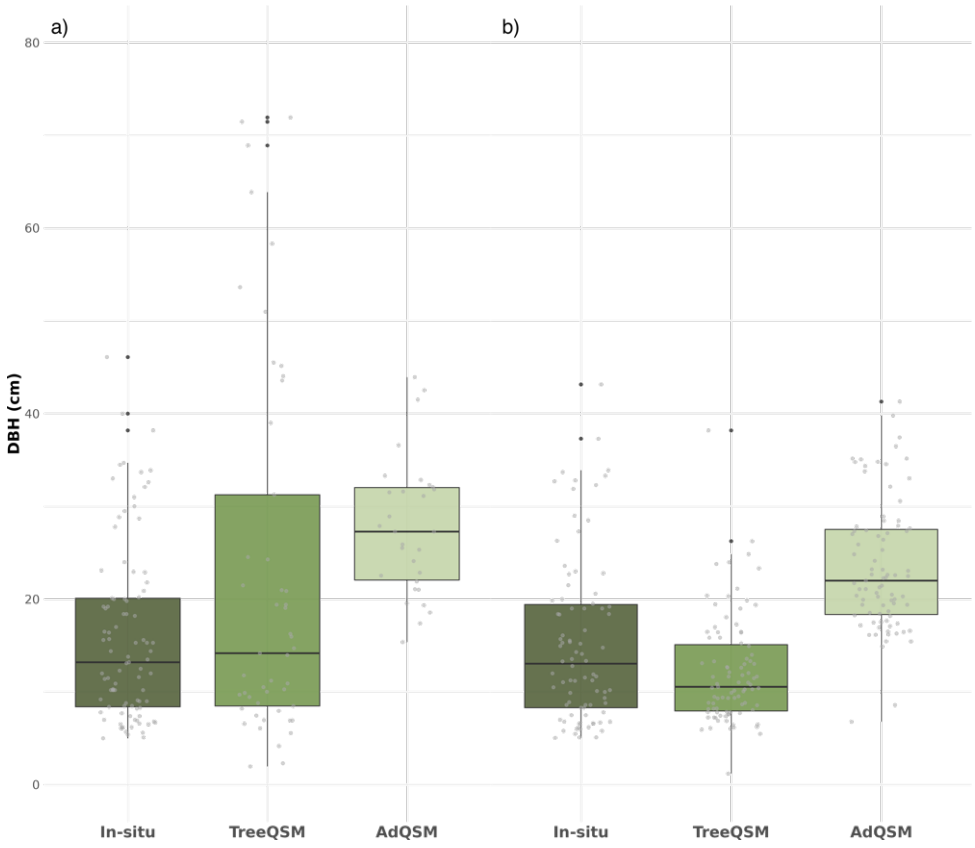



*Figure 3. DBH Distributions of all trees from different approaches in a) leaf-on and b) leaf-off conditions. Seven extreme values (319.04cm, 218.88cm, 11.41cm, 115.45cm, 112.61cm, 105.26cm, 85.955cm) were removed from TreeQSM estimates in a) for visualization purposes w. All other data are included.*

### *3.1.2 Harvested versus Undisturbed sites*

While our sample of trees were all acquired from within the Hullett Wildlife Preserve, a portion of the sample was acquired from a forest that had been harvested and a portion that was acquired from an undisturbed forest (Section 2.1). During the leaf-on data collection, the Harvested site contained 30 trees comprising a mean DBH of 19.92 cm (sd.= 11.97 cm). TreeQSM overestimated the mean DBH (29.97 cm) and obtained a very high standard deviation (32.02 cm). The distribution of TreeQSM-estimated DBH values had little correspondence with in-situ measurements (r = -0.32), a high error and poor model fit (RMSE = 37.6. MAE = 26.7, $R^2$ = 0.10). AdQSM again outperformed TreeQSM. Despite AdQSM obtaining a similarly high mean DBH of 28.30 cm, the standard deviation was smaller 5.82 cm, the correspondence between AdQSM and in-situ results was strong (r = 0.76), error was much lower (RMSE = 5.59, MAE = 3.91) and the model fit was moderate ($R^2$ = 0.57).

Similar results were attained during the leaf-off data collection, where 26 trees were measured in-situ at the same site. The mean DBH of these trees was 17.92 cm (sd = 11.36 cm), which is 2 cm less than observed during the leaf-on season, which is likely due to winter shrinkage (Winget and

Kozlowski 1964, Zweifel & Häsler, 2000) and demonstrates the need to conduct in-situ measurements in concert with remotely sensed data collection to ensure correspondence and accurate results. TreeQSM improved substantially with leaf-off data (mean = 12.03 cm, sd = 5.68 cm, Fig. 4), which more closely aligns with the in-situ measurements, but in contrast to the overprediction of DBH values by TreeQSM during leaf-on, in this case TreeQSM underpredicted DBH values. Regardless, TreeQSM DBH estimates did not correspond well with in-situ measurements (r = -0.37), error was high (RMSE = 15.32, MAE = 12.22), and model fit was low ($R^2$ = 0.14). A better performance was attained by AdQSM, whose DBH values were highly correlated with in-situ measurements (r = 0.97), less error was incurred (RMSE = 9.85, MAE = 8.84) and model fit was very strong ($R^2$ = 0.94).

The Undisturbed Forest site was younger, had a greater tree density (63 trees in 400 $m^2$ plot), and a slightly smaller average DBH (mean = 14.10 cm, sd = 7.60 cm) than the Harvested site. When estimating these DBH values during the leaf-on season, results from TreeQSM were very poor (mean = 47.67 cm, sd = 69.81 cm) with very high error and poor model fit. While AdQSM again performed much better than TreeQSM using leaf-on data, results from AdQSM for this Undisturbed site were not as strong (RMSE = 10.93, MAE = 8.45, r = 0.74, $R^2$ = 0.38) compared to the less dense Harvested site.

During the leaf-off season, the Undisturbed site had 60 live trees with an average DBH of 14.12 cm and a standard deviation of 7.54 cm, almost identical to the leaf-on season. From our point cloud collected at this time, TreeQSM did much better than during leaf-on, slightly under predicting the in-situ mean by 2 cm (mean = 12.23 cm, sd = 5.87 cm) and lower error (RMSE = 9.58, MAE = 7.25), but having poor correspondence on a tree-by-tree basis (r = 0.03) and poor model fit ($R^2$ = 0.00). AdQSM yielded similar error metrics (RMSE = 9.46, MAE = 7.98) to TreeQSM, but these values were better aligned with observations (r = 0.74, $R^2$ = 0.55).

Our comparison of the less dense Harvested forest data to that of the younger, denser, Undisturbed forest showed that AdQSM showed more consistency, correlation, and less error across both forest types and seasons than TreeQSM. We note consistency since in both forest sites AdQSM overpredicted DBH scores compared to in-situ measurements for both leaf-on and leaf-off conditions. However, TreeQSM overpredicted DBH values during leaf-on and under-predicted during leaf-off conditions. While AdQSM outperformed TreeQSM, both QSMs yielded better results in the less dense Harvested forest site compared to the Undisturbed site.

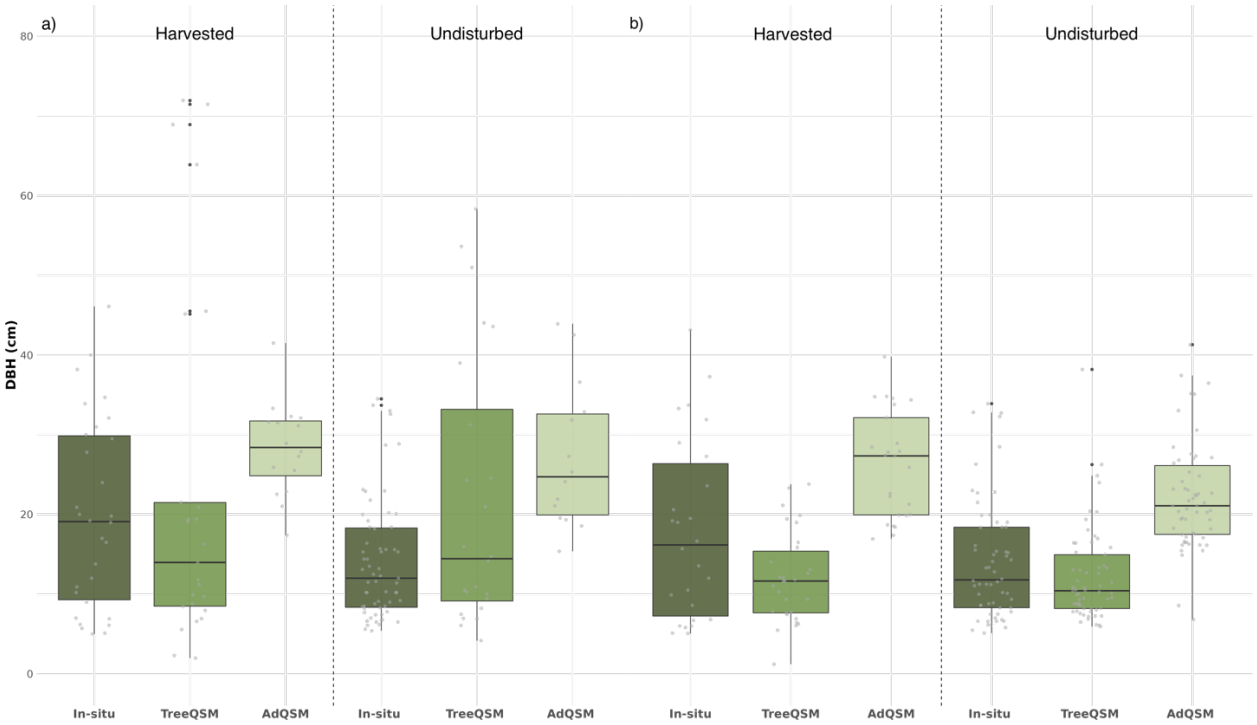



*Figure 4. The DBH distribution for all trees by study site - Harvested and Undisturbed forest in a) leaf-on and b) leaf-off conditions. Extreme values were removed in a) for visualization purposes with their maximum value reaching 80 cm.*

### *3.1.3 DBH Class*

To investigate the potential influence of tree size (via DBH) on model performance, our 93-tree sample during the leaf-on season was divided into eight DBH classes starting with the threshold for tree measurement (5 cm) and increasing up to 45 cm at 5 cm intervals. Our leaf-on in-situ measurements only yielded 1 tree in each of the 35-40 cm and 40-45 cm DBH class intervals, and our leaf-off in-situ measurements only yielded one tree in the 35-40 cm class interval and one tree in the 40-45cm.

Our 900 pts/m$^2$ leaf-on data were not able to observe trees with a DBH less than 10 cm and there was an insufficient number of trees (< 3) to assess DBH classes greater than 35 cm. Within the 10-35 cm range, there was no systematic decrease in error with increasing DBH for TreeQSM, but there was a decrease in error with increasing DBH when AdQSM was used. The two QSM models showed poor correlation with each other (Pearson correlation coefficient ranging from -0.59 to 0.85), demonstrating that they behave differently with the same data. TreeQSM did not perform as well as AdQSM in each of the five DBH intervals and the range of error was much greater for TreeQSM (RMSE = 16.86 - 94.16, MAE = 15.44 - 50.90) than AdQSM (RMSE = 1.30 - 10.66, MAE = 0.93 - 8.59). Partitioning our data by DBH class also showed low correspondence between TreeQSM and in-situ measurements (r = -0.56 - 0.29) and AdQSM showing high correspondence (r = 0.74 - 0.85, Table 5).

*Table 5. Summary of in-situ DBH Class measurements and TreeQSM and AdQSM DBH estimates during leaf-on and leaf-off conditions. Mean and standard deviation (sd.) are reported in centimetres. RMSE = root mean squared error, MAE = mean absolute error, $R^2$ = coefficient of determination.*

| | | In-Situ | | | | | | |
|---|---|---|---|---|---|---|---|---|
| | | Leaf On | | | Leaf Off | | | |
| | | Tree Count | Mean | sd. | Tree Count | Mean | sd. | |
| DBH Class | [5,10) | 31 | 7.18 | 1.27 | 30 | 7.08 | 1.36 | |
| | [10,15) | 20 | 11.90 | 1.47 | 20 | 12.19 | 1.59 | |
| | [15,20) | 16 | 17.18 | 1.66 | 16 | 17.54 | 1.75 | |
| | [20,25) | 10 | 21.60 | 1.54 | 7 | 22.02 | 1.35 | |
| | [25,30) | 4 | 28.71 | 0.70 | 4 | 27.78 | 1.22 | |
| | [30,35) | 9 | 32.83 | 1.59 | 7 | 32.94 | 0.73 | |
| | [35,40) | 1 | 38.20 | - | 1 | 37.30 | - | |
| | [40,45) | 1 | 40.00 | - | 1 | 43.15 | - | |
| | [45,50) | 1 | 46.10 | - | 0 | - | - | |
| | | **TreeQSM** | | | | | | |
| | | Leaf On | | | | Leaf Off | | |
| | | TreeCount | RMSE | MAE | $R^2$ | TreeCount | RMSE | MAE | $R^2$ |
| DBH Class | [5,10) | 8 | 38.25 | 22.73 | 0.35 | 30 | 8.63 | 6.74 | 0.00 |
| | [10,15) | 9 | 59.48 | 44.84 | 0.01 | 19 | 6.91 | 5.01 | 0.10 |
| | [15,20) | 14 | 24.51 | 18.63 | 0.12 | 16 | 7.10 | 5.82 | 0.03 |
| | [20,25) | 10 | 94.19 | 38.19 | 0.08 | 7 | 11.91 | 10.78 | 0.76 |
| | [25,30) | 4 | 17.26 | 15.51 | 0.01 | 4 | 15.79 | 15.34 | 0.67 |
| | [30,35) | 9 | 72.40 | 50.90 | 0.00 | 7 | 22.25 | 21.94 | 0.05 |
| | [35,40) | 1 | - | - | - | 1 | - | - | - |
| | [40,45) | 1 | - | - | - | 1 | - | - | - |
| | | **AdQSM** | | | | | | |
| | | Leaf On | | | | Leaf Off | | |
| | | TreeCount | RMSE | MAE | $R^2$ | TreeCount | RMSE | MAE | $R^2$ |
| DBH Class | [5,10) | 0 | - | - | - | 26 | 12.51 | 11.59 | 0.01 |
| | [10,15) | 3 | 4.58 | 4.47 | 0.65 | 19 | 8.69 | 7.80 | 0.07 |
| | [15,20) | 10 | 10.66 | 7.89 | 0.00 | 16 | 7.75 | 7.33 | 0.08 |
| | [20,25) | 7 | 10.24 | 8.59 | 0.72 | 6 | 9.85 | 7.47 | 0.47 |
| | [25,30) | 3 | 2.69 | 2.12 | 0.55 | 4 | 5.86 | 5.03 | 0.82 |
| | [30,35) | 5 | 1.30 | 0.93 | 0.60 | 7 | 2.25 | 2.14 | 0.20 |
| | [35,40) | 1 | - | - | - | 1 | - | - | - |
| | [40,45) | 1 | - | - | - | 0 | - | - | - |

When we look at our leaf-off season data, we have a slightly higher number of observations ($n_{TreeQSM}$ = 85, $n_{AdQSM}$ = 79) compared to our leaf-on data ($n_{TreeQSM}$ = 59, $n_{AdQSM}$ = 30) due to the increased tree visibility. Analysing our DBH measurements by QSM model with leaf-off data, we again find that, overall, TreeQSM did not perform as well as AdQSM. However, TreeQSM obtained lower RMSE (7.1-8.63) and lower MAE (5.01-6.74) in the three DBH classes between 5-20 cm than was obtained by AdQSM (RMSE = 7.75-12.51, MAE = 7.33-11.59). At DBH classes from 20- 35 cm, TreeQSM performed quite poorly (RMSE = 11.90-22.25, MAE = 10.77-21.94) relative to AdQSM (RMSE = 2.25 - 9.85, MAE = 2.14 - 7.47).

The error metrics and distribution of DBH values by class (Fig. 5) demonstrate that TreeQSM does not perform as well as AdQSM when leaf-on data are used, and TreeQSM only outperforms

AdQSM in the smallest DBH classes (5-10, 10-15, 15-20 cm) when leaf-off data are used. Overall, AdQSM tends to overestimate DBH values, particularly at lower DBH classes, but otherwise consistently achieves lower error and less variation with larger DBH values compared to TreeQSM. While TreeQSM was created with the assumption that leaves would not be included in the point cloud and therefore the reduction in error metrics from leaf-off data was expected, AdQSM experienced several DBH classes that yielded higher error in leaf-off than leaf-on conditions.

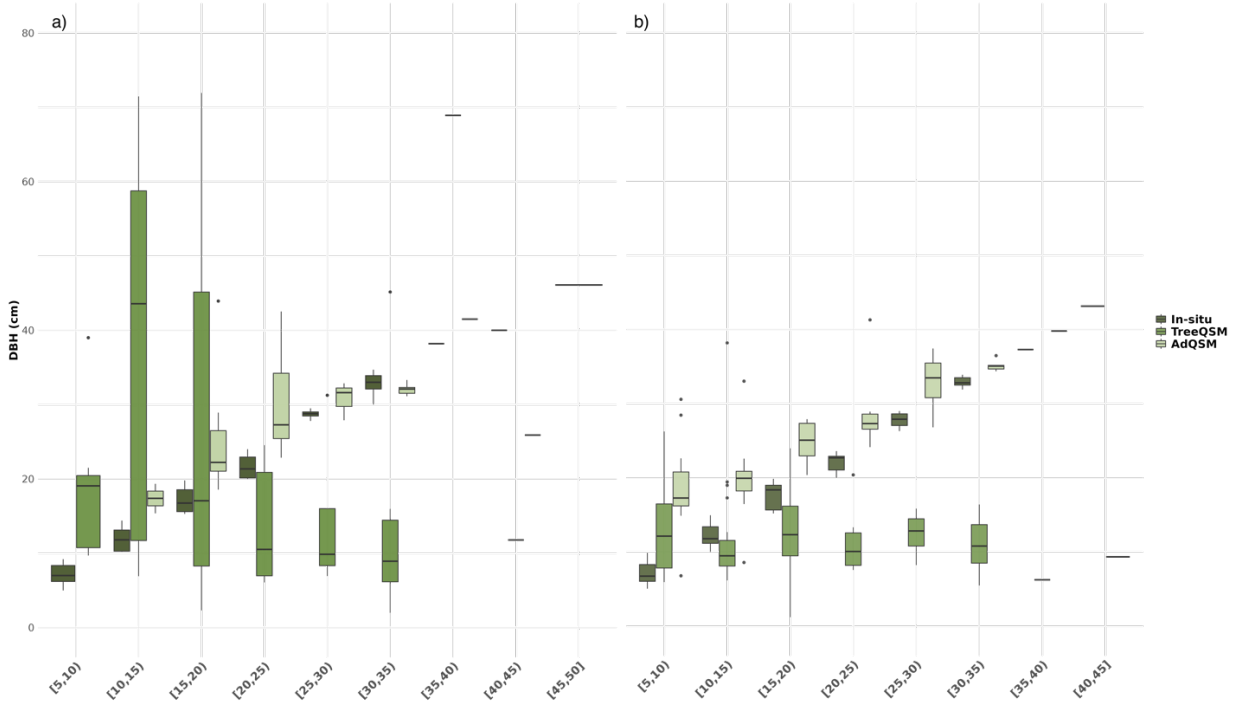



*Figure 5. Distributions of all DBH class from different approaches in a) leaf-on and b) leaf-off conditions. Extreme values were removed in a) for visualization purposes with their maximum value reaching 80 cm.*

## 3.2 Carbon

### *3.2.1 Leaf on versus Leaf off*

In the absence of destructive sampling data, which could serve as a benchmark for assessing the accuracy of quantifying tree biomass and carbon using Remotely Piloted Aircraft LiDAR data and QSM approaches, we utilized a series of allometric equations and i-Tree as reference conditions to evaluate the differences between traditional Allometric Scaling Models (ASMs) and 3D QSM reconstruction models (Table 6). Since the LiDAR data and QSM approaches are unable to capture all trees measured in-situ, we first report on tree count and total estimated carbon stocks and then the distribution of tree carbon values using mean and standard deviation.

*Table 6.Summary of carbon storage (kg) estimation result from allometric equations, i-Tree, TreeQSM and AdQSM in Harvested and Undisturbed forest sites during leaf-on and leaf-off seasons.*

| | | All Tree | | Harvested | | Undisturbed | |
|---|---|---|---|---|---|---|---|
| | | Leaf On | Leaf Off | Leaf On | Leaf Off | Leaf On | Leaf Off |
| Allo.Eq | Total | 9316.52 | 7444.17 | 4764.02 | 3494.69 | 4552.50 | 3949.49 |
| | Tree count | 93 | 86 | 30 | 26 | 63 | 60 |
| | mean | 100.18 | 86.56 | 158.80 | 134.41 | 72.26 | 65.82 |
| | sd | 134.83 | 120.39 | 183.34 | 171.32 | 93.80 | 83.66 |
| i-Tree | Total | 7779.80 | 6282.30 | 4121.60 | 2802.00 | 3658.20 | 3480.30 |
| | Tree count | 93 | 86 | 30 | 26 | 63 | 60 |
| | mean | 83.65 | 73.05 | 137.39 | 107.77 | 58.07 | 58.01 |
| | sd | 128.47 | 106.67 | 189.63 | 155.70 | 74.89 | 73.21 |
| TreeQSM | Total | 84461.48 | 4169.77 | 10846.89 | 1415.09 | 73614.60 | 2754.68 |
| | Tree count | 56 | 85 | 27 | 26 | 29 | 59 |
| | mean | 1508.24 | 49.06 | 401.74 | 54.43 | 2538.43 | 46.69 |
| | sd | 5083.42 | 44.41 | 701.38 | 53.99 | 6929.85 | 39.77 |
| AdQSM | Total | 8046.38 | 12799.98 | 4586.16 | 5284.44 | 3460.22 | 7515.54 |
| | Tree count | 30 | 79 | 16 | 22 | 14 | 57 |
| | mean | 268.21 | 162.03 | 286.64 | 240.20 | 247.16 | 131.85 |
| | sd | 197.85 | 172.75 | 169.51 | 220.55 | 230.81 | 141.42 |

During the leaf-on season, the two ASMs exhibited similar results. The total estimated carbon storage for all trees by allometric equations and i-Tree during the leaf-on season was 9,317 kg and 7,780 kg, respectively. The difference in total carbon is substantial, which is due primarily to the built-in assumption of allometric equations that the trees are in good health. i-Tree has a lower estimate due to the inclusion of dieback as estimated in the field. When we look at the distribution of estimated tree carbon values, the two ASMs had a very high correlation (r = 0.90) and similar average and standard deviation tree-carbon stocks (allometric equations mean = 100kg, sd = 135 kg; i-Tree mean = 84 kg, sd = 128 kg).

Of primary interest is the total carbon stock estimated using the QSMs relative to the ASMs. In leaf-on conditions, the LiDAR data and QSMs were unable to capture and adequately represent a sufficient number of trees. For example, TreeQSM was only able to represent 56 of 93 trees (60%) yet it yielded a total estimated carbon storage of 84,461 kg, which is approximately an order of magnitude greater than the carbon stock estimated by i-Tree. AdQSM represented even fewer trees (n = 30, 32%), which led to a lower total carbon estimate (20,646 kg) than TreeQSM, but it was still much greater than the total carbon stocks estimated by the two ASM approaches.

The average tree carbon from both QSM models were significantly higher than that acquired by the two ASMs. TreeQSM far exceeded the ASM mean values (mean 1508 kg, approximately 15 times greater than the allometric equation and 18 times greater than i-Tree) and produced a very large standard deviation of 5,083 kg. The median value of TreeQSM was very low, indicating that nearly half of the tree samples had very low carbon storage estimates, while a small number of trees with extremely high values significantly inflating the average (Fig. 6). The correlation between the distribution of tree carbon estimates from TreeQSM with the ASMs ($r_{Allo.Eq}$ = 0.08, $r_{i-}$

$_{Tree}$ = 0.14) was weak. While AdQSM also estimated a much greater average tree carbon stock (mean = 268 kg, sd = 198 kg) than the ASMs, AdQSM was only 2-3 times greater and obtained a similar standard deviation. The distribution of individual tree values was moderately correlated ($r_{Allo.Eq}$ = 0.49, $r_{i\text{-}Tree}$ = 0.5) with the ASMs. The differing performances of TreeQSM and AdQSM when compared to the ASMs reflect significant differences in their estimation results, a characteristic also highlighted by the negative correlation (-0.03) between TreeQSM and AdQSM.

Using leaf-off season data, the trends observed during the leaf-on season persisted. Results from our allometric equation approach and i-Tree again provided similar estimates of total and mean carbon storage ($total_{Allo.\ Eq}$ = 7444 kg, $mean_{Allo.\ Eq}$ = 87 kg, $sd_{Allo.\ Eq}$ = 120 kg; $total_{Allo.\ Eq}$ = 6283 kg, $mean_{i\text{-}Tree}$ = 73 kg, $sd_{i\text{-}Tree}$ = 107 kg), and their correlation was very high (r = 0.95). In these leaf-off conditions, the LiDAR data and TreeQSM was able to represent 85 of 86 trees (99%). However, TreeQSM still substantially overestimated total carbon (41,680 kg) and had a substantially lower average tree-carbon storage estimate (49 kg) with a smaller standard deviation (sd = 44 kg) compared to the two ASM approaches. This under estimation contrasts with the very high leaf-on overestimation and demonstrates the inconsistency of TreeQSM. Evaluating the correlation in individual tree-carbon estimates from TreeQSM with the allometric equation approach and i-Tree showed very weak correlations, r = 0.07 and r = 0.08, respectively.

AdQSM with leaf-off LiDAR data acquisition was able to better capture and represent our study area trees (n = 79 or 92% of in-situ measured trees). AdQSM, was more consistent and again over estimated carbon storage relative to the ASMs with a total carbon storage estimate of 12,800 kg. However, in the leaf-off conditions, the average tree-carbon estimate and its standard deviation were closer to that obtained by the ASMs (mean = 162 kg, sd. = 173 kg). Despite the average tree-carbon from AdQSM being almost double that of the ASMs, the distribution of individual tree-carbon estimates was very highly correlated with the allometric equation approach (r = 0.96) and i-Tree (r = 0.91). These results suggest that AdQSM has a greater potential to derive an accurate tree- and forest- carbon estimate compared to TreeQSM, and that further investigation into the factors affecting QSM results such as LiDAR footprint, point density, crown penetration among others is needed.

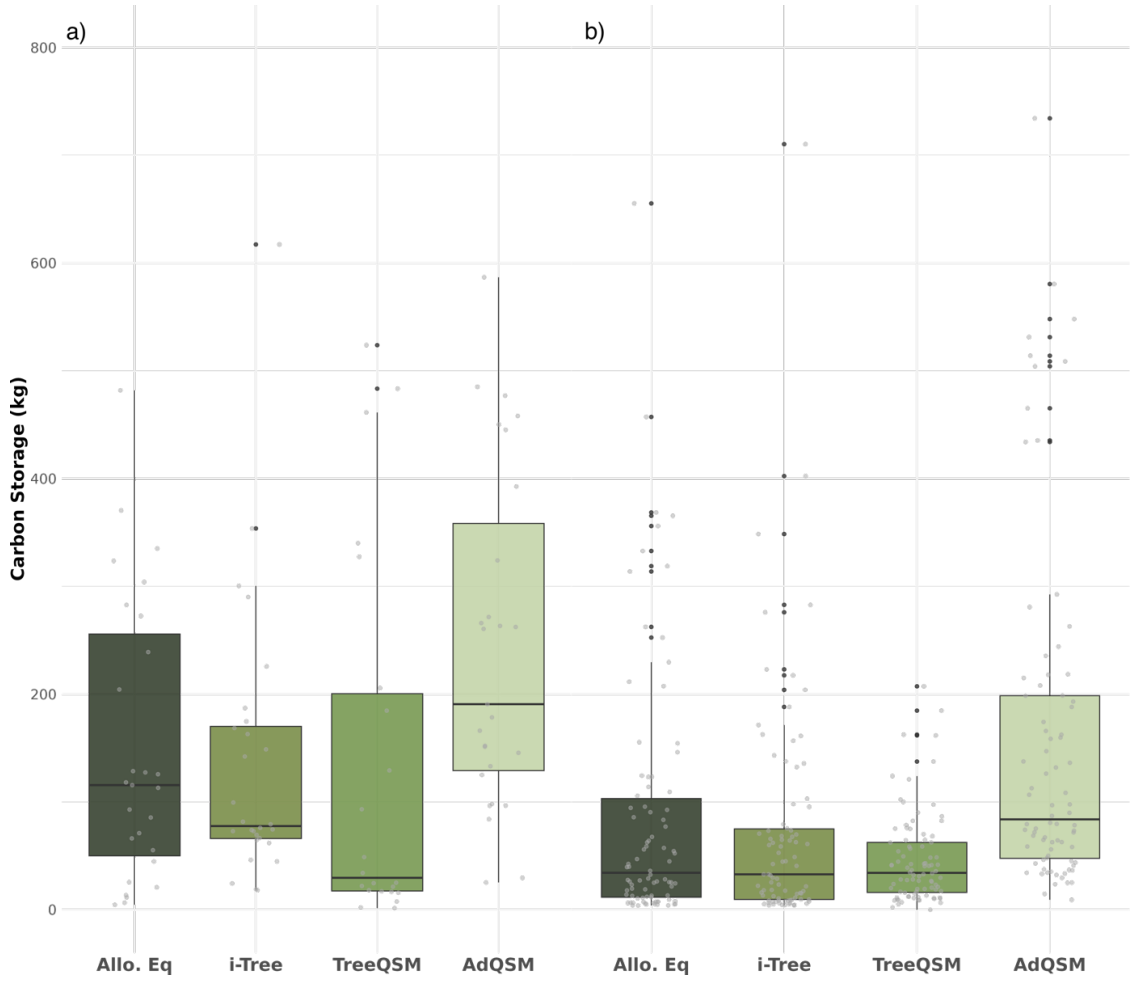



*Figure 6. Carbon storage distribution of all trees from different approaches in a) leaf-on and b) leaf-off conditions. For visualization purposes, 13 extreme values from TreeQSM in a) were removed, as they exceeded 800 kg, with the highest removed value reaching 34,986 kg. But all other data are included.*

### *3.2.2 Harvested versus Undisturbed Forest*

During the leaf-on season, the Harvested forest showed some variability in carbon storage estimates across the different methods. The allometric equation provided a total carbon storage estimate of 4764 kg with a mean tree-carbon estimate of 159 kg (sd = 183 kg), while i-Tree yielded a slightly lower total carbon storage of 4122 kg with mean tree-carbon of 137 kg (sd = 190 kg). A strong Pearson correlation of 0.92 between these two methods suggests that their estimates are closely aligned, as reflected in the overlapping interquartile ranges (Fig.7).

TreeQSM, however, displayed significantly higher variability in tree-carbon estimates (mean = 402 kg, sd. = 701 kg), and yielded with a total carbon storage of 10,847 kg. A maximum tree-carbon value of 2,855 kg far exceeds estimates from the other methods, indicating the presence of outliers that heavily skew TreeQSM results. In addition, a weak correlation of TreeQSM with the allometric equation (r = -0.28) and i-Tree (r = -0.28) indicate that its estimates do not align well with the ASMs. In contrast, AdQSM provided a total carbon storage of 4586 kg, which was within

200 kg of the allometric equations estimate and within 500 kg of the i-Tree estimate (Table 6). The AdQSM mean tree-carbon estimate of 287 kg (sd = 170 kg) was notably higher than the estimates from the allometric equation and i-Tree but was strongly correlated with both ($r_{Allo.\ Eq}$ = 0.81, $r_{i\text{-}Tree}$ = 0.72) suggesting that AdQSM produces a pattern of carbon estimates similar to the ASMs.

In the leaf-off season, the carbon storage estimates for the Harvested forest exhibited a similar pattern with leaf-on season. The allometric equation and i-Tree methods continued to produce closely aligned estimates, with total carbon storage of 3495 kg and 2802 kg, and mean values of 134 kg (sd = 171 kg) and 108 kg (sd = 156 kg), respectively. A Pearson correlation of 0.94 between these methods indicates that their estimates remained consistent, as reflected in the overlapping interquartile ranges (Fig. 7).

TreeQSM provided lower estimates during this season, with a total carbon storage of 1,415 kg, a mean value of 54 kg and a narrower distribution range (sd = 54 kg). The maximum value of 207 kg was significantly lower than those from the other methods, and the weak correlations with the allometric equation (r = -0.20) and i-Tree (r = -0.20) suggest that TreeQSM's estimates were not well aligned with the traditional models during the leaf-off season. AdQSM, on the other hand, produce higher carbon estimates, with a total carbon storage of 5284 kg, a mean value of 240 kg (sd = 221 kg). The correlation between AdQSM and the allometric equation remained very strong (r = 1.00) and the correlation with i-Tree was also very high (r = 0.91), suggesting that AdQSM provides a consistent estimation approach, even if its values are generally higher.

For the Undisturbed forest during the leaf-on season, the allometric equation and i-Tree produced similar carbon storage estimates, with total carbon storage of 4553 kg and 3658 kg, and mean values of 72 kg (sd = 94 kg) and 58 kg (sd = 75 kg), respectively. A strong Pearson correlation of 0.83 between these two methods underscores the consistency and alignment in their estimates. TreeQSM yielded significantly higher carbon storage estimates, with a total carbon storage of 73614 kg, a mean value of 2538 kg and an exceptionally large standard deviation of 6930 kg. The presence of extreme outliers is evident from the maximum value of 34986 kg, contributing to a very broad distribution. The correlations of TreeQSM with the allometric equation (r = 0.18) and i-Tree (r = 0.33) were notably weak. AdQSM provided a total carbon storage of 7516 kg, with a mean tree-carbon estimate of 247 kg (sd = 231 kg), which was 3-5 times higher than those produced by the allometric equation and i-Tree. The correlations between AdQSM and the traditional methods were moderate ($r_{Allo.\ Eq}$ = 0.38, $r_{i\text{-}Tree}$ = 0.30), suggesting that while AdQSM's estimates were higher, they did not fully align with the ASMs in the Undisturbed forest.

When comparing AdQSM and TreeQSM performance in the Undisturbed forest with leaf-on conditions, AdQSM produced more stable and consistent carbon estimates, with a distribution closer to the ASMs, despite being higher overall. TreeQSM, on the other hand, demonstrated significant variability and produced estimates that were often substantially different from those acquired using Allometric Scaling Models (ASMs), as indicated by the weak correlations and broad distributions.

During the leaf-off season, the allometric equation and i-Tree approaches continued to generate closely aligned estimates of total carbon storage of 3950 kg and 3480 kg and mean values of 66 kg (sd = 84 kg) and 58 kg (sd = 73 kg), respectively. A Pearson correlation between the two methods was exceptionally strong at 0.95, showing the consistency in their estimates during the leaf-off season. Among the QSMs, TreeQSM was able to represent 59 of 60 trees (98%) and produced lower total and mean carbon stock estimates than the ASMs (total carbon = 2755 kg, mean = 47 kg; Table 6). However, the correlations with the allometric equation approach (r = 0.09) and i-Tree (r = 0.40) showed a weak association.

AdQSM was able to represent 57 of 60 trees (95%) in leaf-off conditions at the undisturbed site and continued to yield higher carbon storage estimates compared to the ASMs, with a total carbon storage of 7345 kg, a mean of 132 kg (sd = 141 kg). The correlation coefficients between AdQSM and the allometric equation (r = 0.95) and i-Tree (r = 0.95) were both robust, reflecting a strong alignment between AdQSM's estimates and those of the ASMs. In the comparison between AdQSM and TreeQSM, AdQSM consistently provided higher estimates with greater alignment to the allometric based approaches.

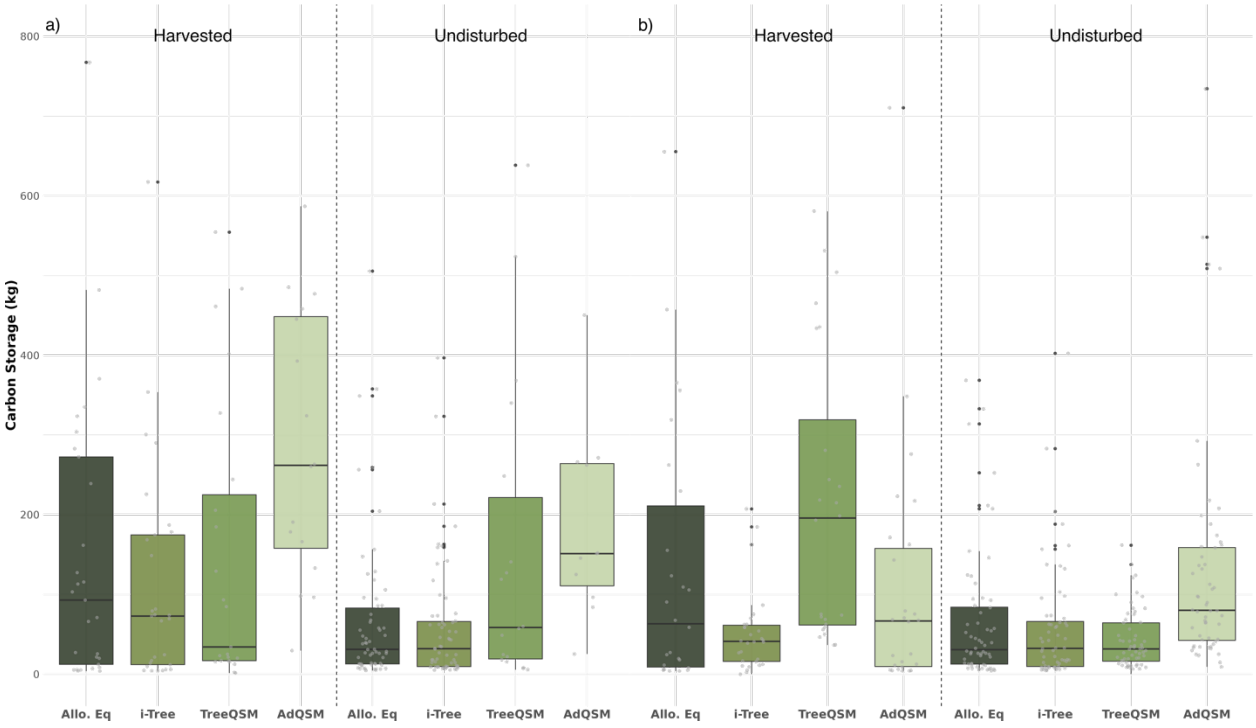



*Figure 7. Carbon storage distribution for all trees by study site, Harvested and Undisturbed forest in a) leaf-on and b) leaf-off conditions. Extreme values were removed in a) for visualization purposes with their maximum value reaching 800 kg.*

*3.2.3 DBH class*

During the leaf-on season, the majority of trees fall within the lower DBH classes, particularly between 10 and 25 cm (Fig. 8). For trees in the [5,10) cm DBH class, the allometric equation and i-Tree showed strong agreement, with a Pearson correlation of 0.89. However, TreeQSM and AdQSM exhibited weak correlations with the allometric equation (r = -0.40 for TreeQSM and no trees for AdQSM) in this class, indicating a divergence in their estimates. Similarly, TreeQSM showed a negative correlation with i-Tree (r = -0.43).

At larger DBH classes, such as [20,25) cm, i-Tree showed moderate correlation with the allometric equation approach (r = 0.47), while TreeQSM and AdQSM exhibited near-zero or negative correlations, particularly TreeQSM, which had a correlation of -0.03 with the allometric equation. This suggests that TreeQSM's estimates do not align well with the ASMs in this DBH range. AdQSM displayed strong correlations with the allometric equation in the [10,15) cm and [20,25) cm classes (r = 1 and r = 0.87, respectively), and similarly, it showed strong correlations with i-Tree (r = 0.99 and r = 0.29). For larger DBH classes, particularly [30,35) cm, the correlation between QSMs and the allometric equation dropped significantly ($r_{TreeQSM}$ = -0.51, $r_{AdQSM}$= -0.18). The correlation between TreeQSM and i-Tree also remained low (r = -0.99), while AdQSM's correlation with i-Tree was slightly better (r = 0.35), though still not strong. The limited number of trees in the higher DBH classes made it challenging to draw strong conclusions, but the data suggests that TreeQSM struggles more with accuracy as DBH increases, particularly in comparison to AdQSM, which, despite some inconsistencies, generally performed better across the range of DBH classes.

In the leaf-off season, the number of trees increased slightly, which allowed for a more informative analysis of the DBH classes. The correlation patterns observed in the leaf-on season persisted, with some notable differences. For the [5,10) cm DBH class, the allometric equation and i-Tree maintained a strong correlation (r = 0.89), similar to the leaf-on season. TreeQSM showed a modest improvement in correlation with the allometric equation (r = 0.28) and with i-Tree (r = 0.09) in this class, suggesting slightly better alignment in the leaf-off data. However, AdQSM's correlation remained weak (r = 0.04 with the allometric equation and r = 0.04 with i-Tree), show that it did not perform as well in this smaller DBH class.

For the [20,25) cm class, TreeQSM and the allometric equation showed moderate correlation (r = 0.61), reflecting better performance than in the leaf-on season. TreeQSM also showed improved correlation with i-Tree (r = 0.49), suggesting a closer alignment with both traditional methods. AdQSM exhibited strong correlations in this class ($r_{Allo.Eq}$= 0.79 and $r_{i\text{-}Tree}$ = 0.3). As DBH increases to [30,35) cm, TreeQSM showed a significant improvement in correlation with the allometric equation (r = 0.45) and i-Tree (r = 0.62), contrasting with its poor performance in the leaf-on season. AdQSM also performed well in this range, with a high correlation of 0.88 with the allometric equation and a moderate correlation with i-Tree (r = 0.44). However, as with the leaf-on season, the data suggests that TreeQSM's estimates are more variable and less reliable as DBH

increases, particularly when compared to AdQSM, which generally showed better alignment with the ASMs.

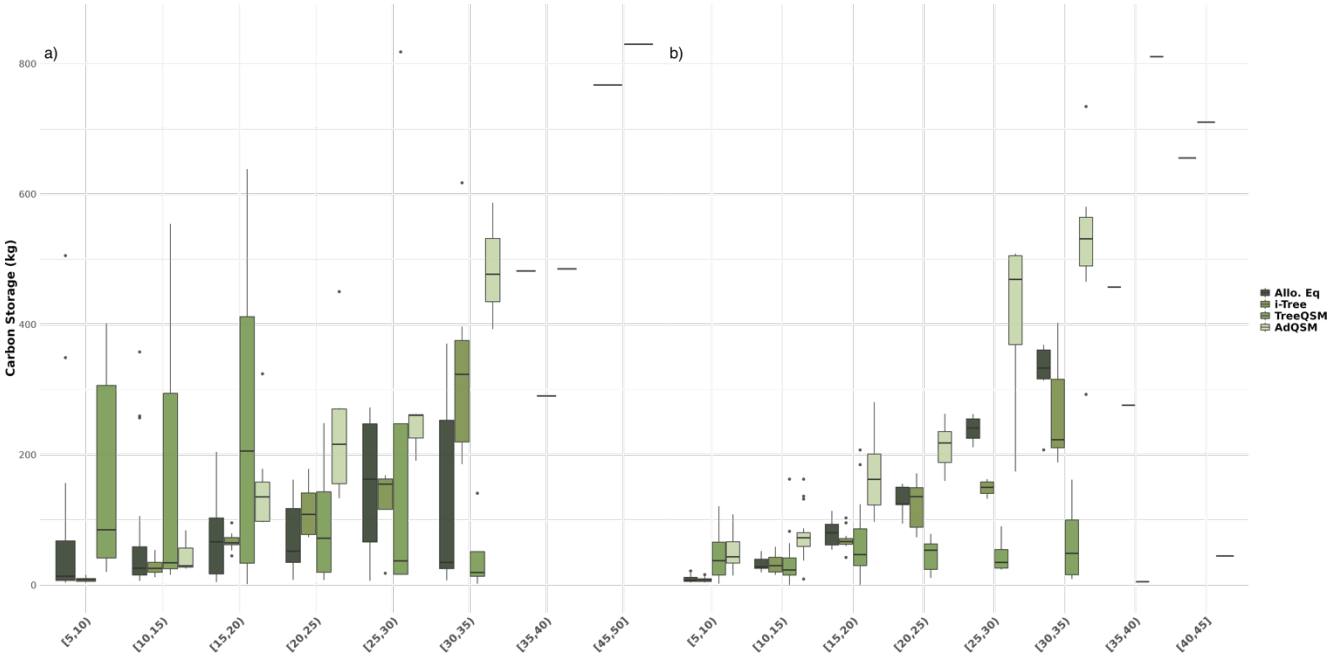



*Figure 8. Carbon storage distribution of all DBH class from different approaches in a) leaf-on and b) leaf-off conditions. 13 extreme values were removed in a) for visualization purposes with their maximum value reaching 800 kg.*

# 4 Discussion

## 4.1 Validation

Our validation efforts of LiDAR and QSM approaches to recreate tree DBH values is a function of our point cloud density 900 pts/m$^2$. Captured from 60 m above ground level, most of these points were intercepted by the tree canopy during leaf-on conditions. Our results demonstrate that with greater penetration of the stem below canopy (during leaf-off) conditions, we were better able to capture DBH. Stem and DBH representation were further improved by LiDAR acquisition in the lower density and larger stemmed Harvested forest than the higher density smaller stemmed Undisturbed forest. Partitioning our data, by DBH class, also demonstrated that larger DBH values were more accurately acquired with our LiDAR data and QSM models than trees with smaller DBH values. The ideal conditions, comprising leaf-off, low density forest (i.e., our Harvested site), and larger trees (DBH >= 20 cm) we were able to acquire mean absolute error (MAE, Table 5) of less than 2.5 cm. The 2-3 cm threshold is significant, since manual measurements of DBH can vary within that range.

Our validation results were based on a tree-by-tree comparison of DBH values. We sought to manually segment trees using CloudCompare (https://www.cloudcompare.org), which was a substantial cost in labour and time. While this approach was used to ensure the highest accuracy of tree identification and representation, leaf-on conditions limited our success with the data collection hardware used. Across the two forest sites, 93 trees were identified in-situ during leaf-on conditions (30 in the Harvested forest and 63 in the Undisturbed forest). However, our manual segmentation was only able to identify 56 trees (60%) of those trees (27 Harvested and 29 Undisturbed). During leaf-off conditions, 86 trees were identified in-situ (26 Harvested and 60 Undisturbed) and we were able to manually segment 85 (99%) of those trees, which highlights the considerable impact of leaf occlusion on the success of tree isolation, especially in denser forests where overlapping trees naturally cause occlusion.

Despite our ability to manually segment tree point clouds, the success rate of 3D tree reconstruction from those point clouds varied between the two QSMs even though they both used identical data. In all conditions, TreeQSM was able to reconstruct more trees than AdQSM, with the greatest difference occurring in the leaf-on conditions (difference of 15 trees) and most similar results during leaf-off conditions in the Undisturbed forest (difference of 2 trees). However, the trees that were represented using AdQSM in almost all conditions yielded lower error and a better model fit than that attained from TreeQSM. While our results suggest that AdQSM should be used moving forward, further investigation is needed to understand how these and other QSMs perform under different flight conditions that affect LiDAR beam divergence or footprint size, horizontal and vertical point density, angle of incidence, number of returns and other flight or sensor parameters that affect data acquisition in addition to environmental conditions such as different forest sites, seasons, and tree growth conditions.

To further illustrate the varying performance of 3D tree reconstruction between TreeQSM and AdQSM under different conditions, we present Figure 9, which shows a side-by side comparison of the LiDAR data and the reconstructions by both QSMs under differing environmental factors. The distinction between good or poor data quality is primarily determined by the completeness and density of the tree stem in the point cloud data. Under good data quality conditions, the point cloud density of tree stem is high, and the points are more continuous, allowing for a more precise and smooth reconstruction of the tree trunk and branches. This results in smaller, tightly connected geometric units that better match the natural form of the tree in the point cloud data.

In contrast, under poor data quality conditions – especially during the leaf-on season – the point cloud around the tree stem become sparse and fragmented due to the occlusion caused by foliage. This data scarcity directly affects the performance of both QSMS. TreeQSM exhibits a visible disjoint in the cylinder connections under poor data conditions. The cylinders are stretched and misaligned due to insufficient point density, leading to a less accurate and coarse representation of the tree structure. In the AdQSM, poor data results in noticeable bends and unnatural curves along the tree stem, deviating from true shape of the tree. This is particularly evident in leaf-on conditions, where the presence of foliage obstruct the visibility of the branch and stem.

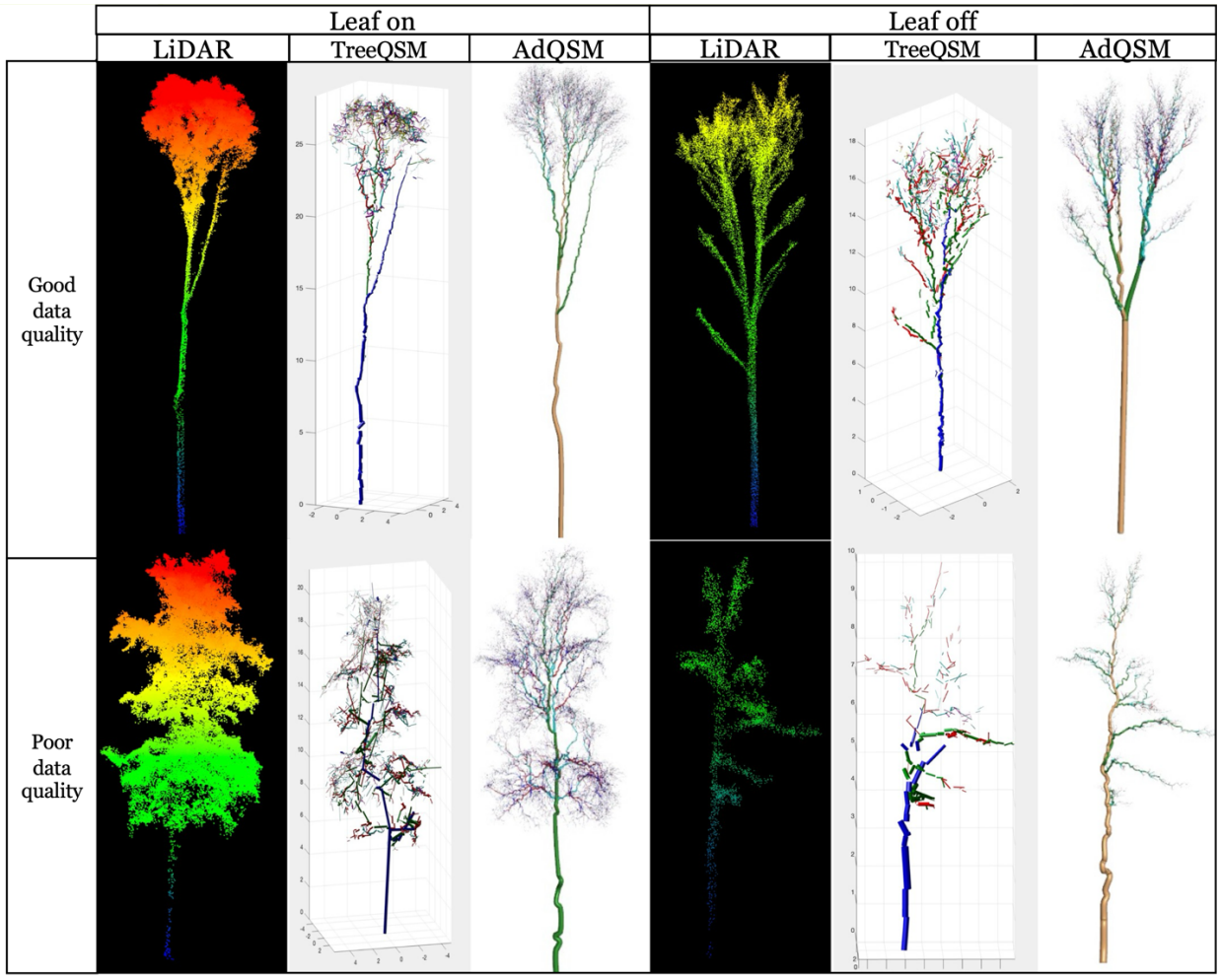



*Figure 9. Comparison of 3D reconstruction model using TreeQSM and AdQSM with LiDAR data under different data quality conditions. The figure illustrates the variation between good and poor data quality in both leaf-on and leaf-off seasons. Point cloud densities for the LiDAR data are as follows: Leaf-on season - Good quality (430 points/m²), Poor quality (340 points/m²); Leaf-off season - Good quality (320 points/m²), Poor quality (280 points/m²).*

### 4.2 Carbon

In the absence of destructive sampling data, we used a compilation of allometric equations and i-Tree for comparison against two Quantitative Structural Modelling (QSM) approaches. The final carbon storage estimates varied significantly depending on the method used. For the traditional Allometric Scaling Models (ASMs), both the allometric equation and i-Tree provided similar and consistent estimates, with total carbon storage ranging from approximately 7,780 kg (i-Tree) to 9,317 kg (allometric equations) during the leaf-on season, and from 6,283 kg (i-Tree) to 7,444 kg (allometric equations) during the leaf-off season.

The allometric equations were harvested from the literature to showcase what a traditional approach would typically yield for tree biomass or carbon. The use of i-Tree as an alternative Allometric Scaling Model (ASM) demonstrated how these results can be adjusted, based on empirical data (e.g., Kaitaniemi and Lintunen, 2008), to accommodate for tree health or other growth limiting factors (e.g., management activities; Nowak, 2021). In fact, the default crown health of i-Tree Eco is 83%, which if applied to our allometric equation results yields 7,733 kg in leaf-on conditions and 6,179 kg in leaf-off conditions – results that are nearly equivalent to i-Tree. While i-Tree has proven incredibly useful and beneficial for many cities (e.g., McPherson et al., 2016; Ma et al., 2021), and research endeavors (e.g., Cimburova and Barton, 2020). i-Tree, like AdQSM, is open access and not open source. Therefore, our allometric equation approach enabled us to pick the equation to be used and understand how it is used, which we are making publicly available upon publication for others to use, contribute to, and build upon.

The carbon estimates obtained from the Quantitative Structure Models (QSMs) differed greatly from those of the ASMs. TreeQSM estimated a total carbon storage of 84,461 kg in the leaf-on season and 41,680 kg in the leaf-off season, which far exceeded the estimates from all other approaches. Furthermore, TreeQSM exhibited substantial variability in tree-carbon and total carbon estimates and unrealistically large sized trees (i.e., outliers). In contrast, results from AdQSM were consistent and carbon estimates were more moderate with a total carbon storage of 20,646 kg in the leaf-on season and 12,800 kg in the leaf-off season, which are higher but much closer to the ASMs. Overestimate of carbon was particularly apparent in the denser (Undisturbed) forest, which has occurred in other research initiatives (Fan et al. 2020). Dense canopy cover and smaller trunk diameters complicate the data acquisition process, making accurate 3D reconstruction more challenging and impacting the model's precision.

TreeQSM and AdQSM, despite their poor correlation, share a common characteristic: both tend to overestimate carbon storage compared to traditional ASMs in a varying degree. By analyzing the 3D reconstruction process and evaluating the results, we have identified several issues related to calibration and validation in both QSMs. TreeQSM offers a high degree of flexibility in operation and produces models with a high level of data completeness. The success of TreeQSM modeling relies on the calibration and fitting of three critical parameters - PatchDiam, the number of models generated, and the selection of the optimal model. However, TreeQSM does not provide a standardized approach for selecting these parameters. Instead, its documentation only offers suggested ranges for parameter settings and numbers of models being generated. This lack of clear standards presents a significant challenge to the accuracy of the results, particularly given the variations in point cloud data density, tree types, and shapes within different study plots. AdQSM, on the other hand, requires less coding expertise and offers better visualization compared to TreeQSM. However, its calibration method is similarly vague. The AdQSM documentation suggests averaging the results from different parameter settings to obtain the final output but does not specify the intervals for these settings or how to handle outliers produced by certain parameters. This lack of explicit standards also impacts the reliability of the results.

### 4.3 Future Avenues for Investigation

Our results demonstrated that AdQSM yielded more consistent results across our three dimensions of analysis (leaf-on vs leaf-off, Harvested vs Undisturbed (i.e., density), and DBH class (i.e., tree size). With a substantial set of in-situ and corresponding Remotely Piloted Aircraft data, it would be possible to capitalize on this consistency through the use of statistical models (e.g., generalized linear models (Picard et al., 2012)) or machine learning (Martínez Prentice et al., 2021). While both approaches can draw statistical or mathematical relationships between the estimated and observed values (e.g., Belgiu & Drăguţ, 2016), artificial intelligence methods such as Schikowski et al., (2018) may be able to densify the point cloud based on a large sample of tree data that could improve the representation of the tree stem and subsequently our DBH measurements and carbon estimates. These same approaches may also be able to take two sets of point cloud data from leaf-on and leaf-off conditions and derive a classification approach for foliage using colour, angle, return number and intensity, and other factors. While foliage classification is being pursued (e.g., Van Den Broeck et al., 2023), it remains a work in progress and could improve tree-carbon estimates, better inform models of tree growth by estimating leaf-area index and could contribute to estimating tree health in lieu of multi- or hyper-spectral data.

In the presented research, trees were manually measured and specifies identification took place in-situ. However, as frequently noted in-situ measurements are not scalable to large spatial extents, our results suggest that it is possible to use LiDAR and QSMs to estimate DBH and tree-carbon using Remotely Piloted Aircraft. However, we did not conduct species classification based on those data. Some have shown that structural data, such as that attained from LiDAR, can be used for species classification (e.g., Tigges et al., 2013). However, most use multi- (Axelsson et al., 2018) or hyper-spectral (Ballanti et al., 2016) data for species classification, with hyper-spectral showing substantially better results. Therefore, it is likely that either hyper-spectral LiDAR or two data collection campaigns (leaf-on and leaf-off) will be required to derive both structural information and species identification for accurate biomass and carbon estimates.

Quantitative Structural Modelling is being increasingly used for 3D tree reconstruction using terrestrial laser scanning (TLS) approaches. However, a variety of other approaches can also be used for 3D tree reconstruction such as voxelization (Hosoi et al., 2013) and stem curve models (Kankare et al., 2013). In a voxelization approach, space is tessellated in three dimensions using cubes known as voxels (i.e., volume pixels). Using trees captured as point clouds, the voxels can be specified in a binary fashion as tree presence or absence depending on the number of points residing in each voxel. Challenges with the voxel approach include determination of resolution and ensuring a water-tight model that also contains volume within the stem where no points reside. In a stem curve approach, the primary goal is to accurately depict the gradual change in diameter from the base to the top of the tree. This method is based on fitting a series of geometric shapes—typically cylinders along the length of the stem to approximate its taper. The stem curve is created by segmenting the tree into cross-sections (Pfeifer et al., 2004), each described by its diameter at

various heights. The stem curve can then be used to estimate tree volume and biomass with great accuracy (Liang et al., 2012), especially when combined with other tree parameters like DBH and height.

Our results suggest that improved accuracy will be attainable with improved point striking of the below canopy stem. Once flight parameters and point-cloud thresholds are attained and known for accurate QSM 3D tree reconstruction, then it will be possible to not only generate accurate carbon estimates across large spatial extents, but we will also be able to use those data to generate novel allometric equations and determine the contexts (e.g., urban versus rural, ecosystem or ecological zone, topography, soil, or other factors) that require localized allometric equations for accurate estimation of tree carbon. Furthermore, given historical challenges with the sample size associated with destructive sampling (e.g., Subedi et al., 2011) and the production of allometric equations in the past, with substantial high-density data, we can assess how accurate allometric equations generated decades ago (Telfer, 1969) are and better represent the size distribution or range of DBH values of species, which is a known issue (Morgenroth et al., 2020).

# 5 Conclusion

The presented research sought to determine the accuracy between Remotely Piloted Aircraft (RPA) acquired LiDAR data and in-situ measurements of diameter at breast height and subsequently what was the degree of correspondence between in-situ-based estimates of biomass and carbon compared to those derived using RPA acquired LiDAR data. To answer these two questions, two quantitative structural models (QSMs, TreeQSM and AdQSM) were used to 3D reconstruct natural forest trees from LiDAR data acquired by an RPA. Results from these models were used to estimate diameter at breast height (DBH) to better understand the capabilities of RPA acquired LiDAR for forestry applications and the potential for these data combined with QSM methods to estimate total tree and forest carbon. To further understand how RPA LiDAR with QSMs compare to in-situ measurements and Allometric Scaling Models, we partitioned the data across three dimensions: leaf phenology (leaf-on versus leaf-off conditions), tree density (an older selectively harvested site and a younger high-density site), and tree size (DBH class). Results showed that AdQSM was more consistent and outperformed TreeQSM in nearly all comparisons across the three dimensions investigated.

Carbon stock estimates derived from the two QSMs were variable when compared to carbon stock estimates derived from traditional Allometric Scaling Models (ASMs). Our results suggest that with a current point cloud density of 900 pts/$m^2$, acquired at nadir (90 degrees downward) using a line scanning sensor acquired in three different directions (see more specifics in Section 2.3), that QSM results cannot be used in lieu of in-situ field measurements for accurate estimation of DBH or aboveground tree and forest carbon. Despite this conclusion, our results demonstrated that under ideal conditions during the leaf-off season, low tree density, and older/larger trees with a DBH between 15-35 cm it is possible to acquire DBH values that are within 2.1-7.5 cm of in-situ DBH

measurements. It has been shown that in-situ DBH measurement errors increase with tree size (Omule 1980), and it is commonly expected that there can be 5% error or more in in-situ DBH measurements (Elzinga 2005). Therefore, it is possible that with more exposure or increased point cloud density, that DBH estimates from RPA-mounted LiDAR will be able to achieve similar results as acquired in-situ.

Recent advancements in remote sensing have significantly contributed to real-time forest modeling and carbon storage estimation, particularly in the field of 3D reconstruction. While most 3D tree reconstruction studies have focused on terrestrial laser scanning, the application of Remotely Piloted Aircraft (RPA)-based LiDAR for 3D tree reconstruction remains a novel endeavour that is challenged by the occlusion of tree stems by leaves and neighbouring trees. However, achieving high-precision 3D reconstruction using RPA-mounted LiDAR has the potential for broader impact than TLS given its ability to cover large spatial extents in a relatively short period of time. Through our investigation of accuracy of DBH and tree carbon estimation we also sought to establish a benchmark for comparison for others and in doing so also provide the first comparison between TreeQSM and AdQSM in a North American temperate deciduous forest.

Due to the effects of leaf and neighbouring tree and branch occlusion, the number of LiDAR points that actually detect the stem is significantly reduced, resulting in incomplete or unidentifiable point clouds for the trunk. The average number of points per tree in this study was $1.5 \cdot 10^4$. In comparison, Van Den Broeck et al. (2023) reported that the number of points per tree captured using TLS in their study on leaf-wood segmentation was $3 \cdot 10^5$, which is 20 times greater than in this study. This suggests that the overall performance of both QSMs was likely constrained by the limitations in point cloud density.

It is clear from the presented research that QSMs show a promising approach to tree carbon stock estimation but their accuracy in the presented research was limited by a point cloud density of 900 pts/m$^2$, much of which was intercepted by the canopy. Increasing point density along the stem is a critical determinant of model accuracy, which in turn determines the precision of non-destructive forest ecosystem aboveground carbon stock estimates. Accurate models are crucial not only for understanding and quantifying the significant role forests play as carbon sinks and in carbon offsetting (Daigneault et al., 2022), but also for providing references for studies on the ecological benefits of forests, such as microclimate regulation and biochemical cycles. The rate at which new Remotely Piloted Aircraft and sensors are being created and deployed is increasing and this equipment are also increasing the amount of data acquisition. For example, in 2024 Riegl released a LiDAR sensor (Ultra 120[23]) that can be mounted on an RPA with a measurement rate of 2.4 million pulses per second, which is 2.3 million more points per second than the Riegl MiniVux 1 used in the presented study. We anticipate significant improvements in data acquisition and 3D tree reconstruction accuracy in the coming decade and how much improvement they provide beyond the presented results at 900 pts/m$^2$.

# Chapter 3

# Future Work

The significance of 3D tree modeling and non-destructive forest carbon storage estimation extends far beyond academic research; it plays a vital role in addressing global environmental challenges and contributing to international frameworks like the Intergovernmental Panel on Climate Change (IPCC) and the United Nations Framework Convention on Climate Change (UNFCCC). These frameworks emphasize the need for accurate, efficient, and scalable methods to monitor, assess, and mitigate climate change (United Nations Framework Convention on Climate Change [UNFCCC], 2015; Intergovernmental Panel on Climate Change [IPCC], 2021-2022). Forest ecosystems, as vital carbon sinks, are at the core of these efforts. Precise forest carbon stock assessments are critical to understanding the dynamics of global carbon cycles, which directly feed into national and international climate policies aimed at reducing greenhouse gas emissions.

The presented research in Chapter 2 represents the initial stage of a broader effort toward the development of advanced, accurate, and non-destructive methods for forest carbon modeling. The blueprint for forest carbon modeling, outlined in documents such as the IPCC's Good Practice Guidance for Land Use, Land-Use Change and Forestry (2003), highlights the necessity of improving existing biomass and carbon stock estimation methods. The ability to use RPAS-based LiDAR data for the extraction of individual tree parameters, as demonstrated in this study, reveals the potential to advance the science of understanding and quantifying tree growth, carbon stocks and sequestration, and the conditions that drive its variability. Likewise, these advances will increase the capacity of landowners and stewards at all levels of scale (e.g., small commercial firms, conservation authorities, government agencies) to use new knowledge and their corresponding tools to address societal needs for carbon quantification to achieve net-zero mandates/goals, natural asset inventory, and the quantification of ecosystem services. However, the presented research is only the beginning and contributes to a broader scientific effort that is rapidly changing. Future research will refine presented techniques to increase their accuracy and applicability across a broader range of forest types and environments.

Once a higher level of validation and accuracy is achieved, the next step is to develop localized Allometric Scaling Models (ASMs), specifically tailored to the forest conditions of the region, using the data obtained from our 3D tree modeling. This localized approach aims to maximize the accuracy of biomass and carbon stock estimations in areas where global or generalized allometric equations may not applicable or produce substantial error. By developing region-specific equations, we forest carbon assessments will be more reflective of local ecological conditions, thereby improving the quality and reliability of data used in environmental planning and policy

decisions. This goal aligns closely with Sustainable Development Goal (SDG) 15: Life on Land, which focuses on sustainably managing forests, combating desertification, and halting biodiversity loss. The localization of these models could be used to support the sustainable management of both natural and urban forests, ultimately contributing to global biodiversity conservation and climate action goals.

In addition to the generation of ASMs, a number of parallel efforts will be required to further improve accuracy and ensure the scalability of tree and forest carbon assessments using LiDAR combined QSM approaches. For example, the manual segmentation used in the presented research is not feasible for large-scale forest modeling. An assessment of existing segmentation methods relative to manual methods is required. The criteria used for validation is typically limited to DBH or tree height. There is a need for a multi-metric validation approach comprising measurements of multiple tree characteristics such as first branch height, canopy area, branch diameters and others. A multi-metric validation approach would not only allow for more comprehensive verification of the QSMs' performance across different dimensions but could also be used to assess the data quality of RPA-based LiDAR in 3D structure modeling. This would maximize the advantages of efficient aerial LiDAR data and enable a non-destructive, in-depth understanding and modeling of various tree structures (e.g., stem, branch, foliage). Furthermore, each of these advances have to be developed and assessed in natural contexts as well as in urban environments.

In the context of urban forests, which are increasingly impacted by human activities, accurate carbon storage estimation becomes even more critical. Urban forests are not only vital for carbon sequestration but also provide numerous ecological services that directly improve the quality of life in cities, from air purification to temperature regulation. The IPCC's Sixth Assessment Report (2021) highlights the growing importance of urban ecosystems in mitigating climate change, and the presented research aims to contribute to this body of knowledge by enabling more accurate assessments of urban tree carbon stocks. As cities expand and urbanization accelerates, understanding the carbon dynamics of urban forests becomes essential to meeting the needs of urban populations while maintaining ecological balance. SDG 11: Sustainable Cities and Communities, which seeks to make cities inclusive, safe, resilient, and sustainable, also emphasizes the role of urban forests in this process.

This study began by addressing the challenges of modeling trees in highly complex forest environments, where dense canopy structures and uneven terrain make individual tree parameter extraction extremely difficult. However, by starting with the most challenging conditions in natural forests, we have laid the groundwork for applying these methods to simpler environments - urban forests. The knowledge gained from this research will enable us to apply these advanced modeling techniques to urban forests, where trees are often more spatially isolated, have broader crowns, and are less affected by occlusion when using aerial LiDAR. This transition will allow us to better assess carbon stocks in urban settings, which are more directly influenced by human-induced factors such as pollution, land use change, and climate variability.

3D tree modeling is crucial not only for advancing our understanding of tree structure but also for automating the extraction of tree parameters in a time-efficient, resource-saving manner. This capability is invaluable for the sustainable management of both natural and urban forests. By minimizing the need for labor-intensive fieldwork while maintaining high accuracy, we can scale our efforts to large areas and diverse ecosystems. As international frameworks continue to call for more comprehensive and accurate forest carbon accounting, the methods developed in this study can offer a baseline for comparison and inform those seeking to conduct similar work about the accuracy of the equipment used and its impact on the measurement of tree and forest carbon. Systematic improvements can contribute to the global effort to measure, monitor, model, and protect the world's forests.

# References


Aguilar, F. J., Nemmaoui, A., Peñalver, A., Rivas, J. R., & Aguilar, M. A. (2019). Developing Allometric Equations for Teak Plantations Located in the Coastal Region of Ecuador from Terrestrial Laser Scanning Data. *Forests*, 10(12), 1050. https://doi.org/10.3390/f10121050

Annighöfer, P., Ameztegui, A., Ammer, C., Balandier, P., Bartsch, N., Bolte, A., Coll, L., Collet, C., Ewald, J., Frischbier, N., Gebereyesus, T., Haase, J., Hamm, T., Hirschfelder, B., Huth, F., Kändler, G., Kahl, A., Kawaletz, H., Kuehne, C., … Mund, M. (2016). Species-Specific and Generic Biomass Equations For Seedlings and Saplings of European Tree Species. *European Journal of Forest Research*, 135(2), 313–329. https://doi.org/10.1007/s10342-016-0937-z

Australia's State of the Forests Report 2018. (2018).

Axelsson, A., Lindberg, E., & Olsson, H. (2018). Exploring Multispectral ALS Data for Tree Species Classification. *Remote Sensing*, 10(2), 183. https://doi.org/10.3390/rs10020183

Ballanti, L., Blesius, L., Hines, E., & Kruse, B. (2016). Tree Species Classification Using Hyperspectral Imagery: A Comparison of Two Classifiers. *Remote Sensing*, 8(6), 445. https://doi.org/10.3390/rs8060445

Bansod, B., Singh, R., Thakur, R., & Singhal, G. (2017). A Comparison Between Satellite Based and Drone Based Remote Sensing Technology to Achieve Sustainable Development: A Review. *Journal of Agriculture and Environment for International Development (JAEID)*, 111(2). https://doi.org/10.12895/jaeid.20172.690

Bartlett, J., Rusch, G.M., Kyrkjeeide, M.O., Sandvik, H. & Nordén, J. 2020. Carbon storage in Norwegian Ecosystems (revised edition). NINA Report 1774b. *Norwegian Institute for Nature Research.*

Belgiu, M., & Drăguţ, L. (2016). Random forest in remote sensing: A review of applications and future directions. *ISPRS Journal of Photogrammetry and Remote Sensing*, 114, 24-31. https://doi.org/10.1016/j.isprsjprs.2016.01.011

Bienert, A. *et al.* (2014) 'A voxel-based technique to estimate the volume of trees from Terrestrial Laser Scanner Data', *The International Archives of the Photogrammetry, Remote Sensing and Spatial Information Sciences*, XL–5, pp. 101–106. doi:10.5194/isprsarchives-xl-5-101-2014.

Brede, B., Calders, K., Lau, A., Raumonen, P., Bartholomeus, H., Herold, M., & Kooistra, L. (2019). Non-Destructive Tree Volume Estimation Through Quantitative Structure Modelling: Comparing UAV Laser Scanning with Terrestrial LiDAR. *Remote Sensing of Environment*, 233. https://doi.org/10.1016/j.rse.2019.111355

Brede, B., Terryn, L., Barbier, N., Bartholomeus, H. M., Bartolo, R., Calders, K., Derroire, G., Krishna Moorthy, S. M., Lau, A., Levick, S. R., Raumonen, P., Verbeeck, H., Wang, D., Whiteside, T., Van Der Zee, J., & Herold, M. (2022). Non-Destructive Estimation of Individual Tree Biomass: Allometric Models, Terrestrial And UAV Laser Scanning. *Remote Sensing of Environment*, 280, 113180. https://doi.org/10.1016/j.rse.2022.113180

Brown, S., & Lugo, A. E. (1982). The Storage and Production of Organic Matter in Tropical Forests and Their Role in the Global Carbon Cycle. *Biotropica*, 14(3), 161. https://doi.org/10.2307/2388024

Calders, K., Newnham, G., Burt, A., Murphy, S., Raumonen, P., Herold, M., Culvenor, D., Avitabile, V., Disney, M., Armston, J., & Kaasalainen, M. (2015). Non-destructive Estimates of Above-Ground Biomass Using Terrestrial Laser Scanning. *Methods in Ecology and Evolution*, 6(2), 198–208. https://doi.org/10.1111/2041-210X.12301

Calvo, E. (2007). Climate Change 2007: Mitigation. *Contribution of Working Group III to the Fourth Assessment Report of the Intergovernmental Panel on Climate Change.*

Canadell, J. G., & Raupach, M. R. (2008). Managing Forests for Climate Change Mitigation. *Science*, 320(5882), 1456–1457. https://doi.org/10.1126/science.1155458

Case, B. S., & Hall, R. J. (2008). Assessing Prediction Errors of Generalized Tree Biomass and Volume Equations for The Boreal Forest Region of West-Central Canada. *Canadian Journal of Forest Research*, 38(4), 878–889. https://doi.org/10.1139/x07-212

Carpenter, E. M. (1985). Brief History and Discussion of Biomass Estimation for Timber Tree Species. In Proceedings--*Growth and Yield and Other Mensurational Tricks: A Regional*

*Technical Conference*, Logan, Utah, November 6-7, 1984 (Vol. 193, p. 72). US Department of Agriculture, Forest Service, Intermountain Research Station.

Catchpole, W. R., & Wheeler, C. J. (1992). Estimating Plant Biomass: A Review of Techniques. *Australian Journal of Ecology*, 17(2), 121–131. https://doi.org/10.1111/j.1442-9993.1992.tb00790.x

Chaturvedi, A.N. and Khanna, L.S. (1994) *Forest mensuration*. Dehra Dun: International Book Distributors.

Chave, J., Davies, S. J., Phillips, O. L., Lewis, S. L., Sist, P., Schepaschenko, D., Armston, J., Baker, T. R., Coomes, D., Disney, M., Duncanson, L., Hérault, B., Labrière, N., Meyer, V., Réjou-Méchain, M., Scipal, K., & Saatchi, S. (2019). Ground Data are Essential for Biomass Remote Sensing Missions. *Surveys in Geophysics*, 40(4), 863–880. https://doi.org/10.1007/s10712-019-09528-w

Chow, P.; Rolfe, G.L. (1989). Carbon and Hydrogen Contents of Short-Rotation Biomass of Five Hardwood Species. *Wood and Fiber Science*. 21(1): 30-36

Cimburova, Z., & Barton, D. N. (2020). The Potential of Geospatial Analysis and Bayesian Networks to Enable i-Tree Eco Assessment of Existing Tree Inventories. *Urban Forestry & Urban Greening*, 55, 126801. https://doi.org/10.1016/j.ufug.2020.126801

City of Melbourne. (2012). *Urban Forest Strategy: Making A Great City Greener 2012-2032*.

*Climate change 2007: Mitigation of climate change: Contribution of Working Group III to the Fourth Assessment Report of the intergovernmental panel on climate change*. Cambridge: Cambridge University Press.

Daigneault, A., Baker, J. S., Guo, J., Lauri, P., Favero, A., Forsell, N., Johnston, C., Ohrel, S. B., & Sohngen, B. (2022). How The Future of The Global Forest Sink Depends on Timber Demand, Forest Management, And Carbon Policies. *Global Environmental Change*, 76, 102582. https://doi.org/10.1016/j.gloenvcha.2022.102582

de Tanago, J., Lau, A., Bartholomeus, H., Herold, M., Avitabile, V., Raumonen, P., Martius, C., Goodman, R., Disney, M., Manuri, S., Burt, A., & Calders, K. (2018). Estimation of Above-Ground Biomass of Large Tropical Trees with Terrestrial LiDAR. *Methods in Ecology and Evolution*, 9(2), 223–234. https://doi.org/10.1111/2041-210X.12904

Disney, M., Vicari, M., Burt, A., Calders, K., Lewis, S., Raumonen, P., & Wilkes, P. (2018). Weighing Trees with Lasers: Advances, Challenges and Opportunities. *Interface Focus*, 8(2). https://doi.org/10.1098/rsfs.2017.0048

Eggleston HS, Buendia L, Miwa K, Ngara T, Tanabe K. (2006). IPCC Guidelines for National Greenhouse Gas Inventories Volume - IV Agriculture, Forestry and other and-use. *Institute of Global Environmental Strategies (IGES)*, Hayama, Japan.

Elzinga, C., Shearer, R. C., & Elzinga, G. (2005). Observer Variation in Tree Diameter Measurements. *Western Journal of Applied Forestry*, 20(2), 134–137. https://doi.org/10.1093/wjaf/20.2.134

Forestry department. (2015). *FAO assessment of forests and carbon stocks*, 1990-2015. FAO. https://www.fao.org/documents/card/en/c/2e2f045a-e39b-4b11-965c-/

Girard, J. W., & Gevorkiantz, S. R. (1939). *Timber cruising*. Forest Service, US Department of Agriculture.

Gower, S. T., Krankina, O., Olson, R. J., Apps, M., Linder, S., & Wang, C. (2001). Net Primary Production and Carbon Allocation Patterns of Boreal Forest Ecosystems. *Ecological Applications*, 11(5), 1395–1411. https://doi.org/10.1890/1051-0761(2001)011[1395:NPPACA]2.0.CO;2

Gower, S. T. (2003). Patterns and Mechanisms of the Forest Carbon Cycle. *Annual Review of Environment and Resources*, 28(1), 169–204. https://doi.org/10.1146/annurev.energy.28.050302.105515

Hackenberg, J., Spiecker, H., Calders, K., Disney, M., & Raumonen, P. (2015). SimpleTree—An Efficient Open Source Tool to Build Tree Models from TLS Clouds. *Forests*, 6(12), 4245–4294. https://doi.org/10.3390/f6114245

Hauglin, M., Astrup, R., Gobakken, T., & Næsset, E. (2013). Estimating Single-Tree Branch Biomass of Norway Spruce with Terrestrial Laser Scanning Using Voxel-Based and Crown Dimension Features. *Scandinavian Journal of Forest Research*, 28(5), 456–469. https://doi.org/10.1080/02827581.2013.777772

Hosoi, F., Nakai, Y., & Omasa, K. (2013). 3-D Voxel-Based Solid Modeling of A Broad-Leaved Tree For Accurate Volume Estimation Using Portable Scanning LiDAR. *ISPRS Journal*

*of Photogrammetry and Remote Sensing*, 82, 41–48. https://doi.org/10.1016/j.isprsjprs.2013.04.011

Hojer, A.G. (1903). Tallens och granens tillvaxt. *Biharg till Fr. Lovén*. Om vara barrskogar. Stockholm, Norway.

Houghton, E. (1996). *Climate Change 1995: The Science of Climate Change: Contribution of Working Group I to the Second Assessment Report of the Intergovernmental Panel on Climate Change, 2*. Cambridge: Cambridge University Press

Intergovernmental Panel on Climate Change. (2003). *Good practice guidance for land use, land-use change and forestry. Institute for Global Environmental Strategies (IGES) for the IPCC*.

Intergovernmental Panel on Climate Change. (2021-2022). *Sixth Assessment Report (AR6).* https://www.ipcc.ch/assessment-report/ar6/

Jaafar, H. A., Meng, X., & Sowter, A. (2018). Terrestrial Laser Scanner Error Quantification for The Purpose of Monitoring. *Survey Review*, 50(360), 232–248. https://doi.org/10.1080/00396265.2016.1259721

Jucker, T., Caspersen, J., Chave, J., Antin, C., Barbier, N., Bongers, F., Dalponte, M., van Ewijk, K. Y., Forrester, D. I., Haeni, M., Higgins, S. I., Holdaway, R. J., Iida, Y., Lorimer, C., Marshall, P. L., Momo, S., Moncrieff, G. R., Ploton, P., Poorter, L., … Coomes, D. A. (2017). Allometric Equations for Integrating Remote Sensing Imagery into Forest Monitoring Programmes. *Global Change Biology*, 23(1), 177–190. https://doi.org/10.1111/gcb.13388

Kaartinen, H., Hyyppä, J., Yu, X., Vastaranta, M., Hyyppä, H., Kukko, A., Holopainen, M., Heipke, C., Hirschmugl, M., Morsdorf, F., Næsset, E., Pitkänen, J., Popescu, S., Solberg, S., Wolf, B. M., & Wu, J.-C. (2012). An International Comparison of Individual Tree Detection and Extraction Using Airborne Laser Scanning. *Remote Sensing*, 4(4), 950–974. https://doi.org/10.3390/rs4040950

Kaitaniemi, P., & Lintunen, A. (2008). Precision of Allometric Scaling Equations for Trees Can Be Improved by Including the Effect Of Ecological Interactions. *Trees*, 22(4), 579–584. https://doi.org/10.1007/s00468-008-0218-7

Kankare, V., Holopainen, M., Vastaranta, M., Puttonen, E., Yu, X., Hyyppä, J., Vaaja, M., Hyyppä, H., & Alho, P. (2013). Individual Tree Biomass Estimation Using Terrestrial Laser Scanning. *ISPRS Journal of Photogrammetry and Remote Sensing*, 75, 64–75. https://doi.org/10.1016/j.isprsjprs.2012.10.003

Keith, H., Mackey, B. G., & Lindenmayer, D. B. (2009). Re-evaluation of Forest Biomass Carbon Stocks and Lessons From The World's Most Carbon-Dense Forests. *Proceedings of the National Academy of Sciences*, 106(28), 11635–11640. https://doi.org/10.1073/pnas.0901970106

Kim, C., Jeong, J., Kim, R.-H., Son, Y.-M., Lee, K. H., Kim, J.-S., & Park, I.-H. (2011). Allometric Equations and Biomass Expansion Factors of Japanese Red Pine on the Local Level. *Landscape and Ecological Engineering*, 7(2), 283–289. https://doi.org/10.1007/s11355-010-0131-2

Kurz, W. A., & Apps, M. J. (2006). Developing Canada's National Forest Carbon Monitoring, Accounting and Reporting System to Meet the Reporting Requirements of the Kyoto Protocol. *Mitigation and Adaptation Strategies for Global Change*, 11(1), 33–43. https://doi.org/10.1007/s11027-006-1006-6

Lau, A., Bentley, L. P., Martius, C., Shenkin, A., Bartholomeus, H., Raumonen, P., Malhi, Y., Jackson, T., & Herold, M. (2018). Quantifying Branch Architecture of Tropical Trees Using Terrestrial Lidar and 3D Modelling. *Trees,* 32(5), 1219–1231. https://doi.org/10.1007/s00468-018-1704-1

Lau, A., Calders, K., Bartholomeus, H., Martius, C., Raumonen, P., Herold, M., Vicari, M., Sukhdeo, H., Singh, J., & Goodman, R. (2019). Tree Biomass Equations from Terrestrial LiDAR: A Case Study in Guyana. *Forests*, 10(6), 527. https://doi.org/10.3390/f10060527

Liang, X., Kankare, V., Hyyppä, J., Wang, Y., Kukko, A., Haggrén, H., Yu, X., Kaartinen, H., Jaakkola, A., Guan, F., Holopainen, M., & Vastaranta, M. (2016). Terrestrial Laser Scanning in Forest Inventories. *ISPRS Journal of Photogrammetry and Remote Sensing*, 115, 63–77. https://doi.org/10.1016/j.isprsjprs.2016.01.006

Lin, J., Chen, D., Wu, W., & Liao, X. (2022). Estimating Aboveground Biomass of Urban Forest Trees with Dual-Source UAV Acquired Point Clouds. *Urban Forestry & Urban Greening*, 69. https://doi.org/10.1016/j.ufug.2022.127521

Liu, C., & Wang, S. (2022). Estimating Tree Canopy Height in Densely Forest-Covered Mountainous Areas Using Gedi Spaceborne Full-Waveform Data. *ISPRS Annals of the Photogrammetry, Remote Sensing and Spatial Information Sciences*, V-1–2022, 25–32. https://doi.org/10.5194/isprs-annals-V-1-2022-25-2022

Losi CJ, Siccama TG, Condit R, Morales JE (2003) Analysis of Alternative Methods for Estimating Carbon Stock in Young Tropical Plantations. *Forest Ecology and Management* 184: 355-368.

Management Plan. *Ontario Ministry of Natural Resources – Guelph District*. 25pp.

McHale, M. R. (2008). Volume Estimates of Trees with Complex Architecture from Terrestrial Laser Scanning. *Journal of Applied Remote Sensing*, 2(1), 023521. https://doi.org/10.1117/1.2939008

Nabuurs, G.J., Masera, O., et al., (2007) Forestry, in Climate Change 2007: Mitigation. In: Metz, B., Davidson, O.R., Bosch, P.R., Dave, R. and Meyer, L.A., Eds., *Contribution of working Group III to the Fourth Assessment Report of the Intergovernmental Panel on Climate Change*, Cambridge, Cambridge University Press, 541-584.

Nowak, D. J. (2021). *Understanding i-Tree: 2021 Summary of programs and methods* (NRS-GTR-200-2021; p. NRS-GTR-200-2021). U.S. Department of Agriculture, Forest Service, Northern Research Station. https://doi.org/10.2737/NRS-GTR-200-2021

Ma, J., Li, X., Baoquan, J., Liu, X., Li, T., Zhang, W., & Liu, W. (2021). Spatial Variation Analysis of Urban Forest Vegetation Carbon Storage and Sequestration in Built-up Areas of Beijing Based on i-Tree Eco and Kriging. *Urban Forestry & Urban Greening*, 66, 127413. https://doi.org/10.1016/j.ufug.2021.127413

Malhi, Y., Meir, P., & Brown, S. (2002). Forests, Carbon and Global Climate. Philosophical Transactions of the Royal Society of London. *Series A: Mathematical, Physical and Engineering Sciences*, 360(1797), 1567–1591. https://doi.org/10.1098/rsta.2002.1020

Martínez Prentice, R., Villoslada Peciña, M., Ward, R. D., Bergamo, T. F., Joyce, C. B., & Sepp, K. (2021). Machine Learning Classification and Accuracy Assessment from High-Resolution Images of Coastal Wetlands. *Remote Sensing*, 13(18), 3669. https://doi.org/10.3390/rs13183669

McPherson, E. G., Van Doorn, N. S., & Peper, P. J. (2016). *Urban Tree Database and Allometric Equations* (PSW-GTR-253; p. PSW-GTR-253). U.S. Department of Agriculture, Forest Service, Pacific Southwest Research Station. https://doi.org/10.2737/PSW-GTR-253

Morgenroth, J., Nowak, D., & Koeser, A. (2020). DBH Distributions in America's Urban Forests—An Overview of Structural Diversity. *Forests*, 11(2), 135. https://doi.org/10.3390/f11020135

Omule, S. A. Y. (1980). Personal Bias in Forest Measurements. *The Forestry Chronicle*, 56(5), 222–224. https://doi.org/10.5558/tfc56222-5

Ontario Ministry of Natural Resources, 1985. *Hullett Provincial Wildlife Area Management Plan*. Ontario Ministry of Natural Resources.

Ontario Ministry of Natural Resources, 2008. *Hullett Provincial Wildlife Area Wildlife Habitat Management Plan*. Ontario Ministry of Natural Resources.

PPR, 2020. Urban Forest Action Plan: 2020 Implementation Update. *Portland Parks & Recreation*, pp. 12. URL https://www.portland.gov/trees/documents/2020-urban-forest-action-plan-implementation-update/download (Last accessed on 2023-10-18)

Picard, N., Saint-André, L., & Henry, M. (2012). *Manual for building tree volume and biomass allometric equations: From field measurement to prediction*. Food and Agriculture Organization (FAO).

Ormerod, D.W. 1973. A simple bole model. *For. Chron*. 49(3): 136–138. doi:10.5558/tfc49136-3.

Puric-Mladenovic, D. and Kenney, W.A. 2015. Vegetation Sampling Protocol (VSP). *The VSP Field Inventory and Monitoring Pocket Guide. Version 1 (May 2015)*. Ontario Ministry of Natural

Ravindranath, N. H., & Ostwald, M. (2008). Carbon Inventory Methods Handbook for Greenhouse Gas Inventory, Carbon Mitigation and Roundwood Production Projects. *Springer Netherlands*. https://doi.org/10.1007/978-1-4020-6547-7

Ravindranath, N. H., & Ostwald, M. (Eds.). (2008). Methods for Estimating Above-Ground Biomass. In Carbon Inventory Methods Handbook for Greenhouse Gas Inventory, Carbon Mitigation and Roundwood Production Projects (pp. 113–147). *Springer Netherlands*. https://doi.org/10.1007/978-1-4020-6547-7_10

Raumonen, P., Casella, E., Calders, K., Murphy, S., Åkerblom, M., & Kaasalainen, M. (2015). Massive-Scale Tree Modelling from TLS Data. *ISPRS Annals of the Photogrammetry, Remote Sensing and Spatial Information Sciences*, II-3/W4, 189–196. https://doi.org/10.5194/isprsannals-II-3-W4-189-2015

Raumonen, P. (n.d.). Instructions for MATLAB-software TreeQSM, version 2.4.

Raumonen, P., Kaasalainen, M., Åkerblom, M., Kaasalainen, S., Kaartinen, H., Vastaranta, M., Holopainen, M., Disney, M., & Lewis, P. (2013). Fast Automatic Precision Tree Models from Terrestrial Laser Scanner Data. *Remote Sensing*, 5(2), 491–520. https://doi.org/10.3390/rs5020491

Ravindranath, N. H., & Ostwald, M. (2008). Carbon Inventory Methods Handbook for Greenhouse Gas Inventory, Carbon Mitigation and Roundwood Production Projects. *Springer Netherlands*. https://doi.org/10.1007/978-1-4020-6547-7

Resources and Forestry, Science and Research Branch and The Faculty of Forestry, University of Toronto. 102pp.

Rodger AS (1993) The Carbon Cycle and Global Forest Ecosystem. *Water, Air and Soil Pollution* 70: 295-307.

Roxburgh, S. H., Paul, K. I., Clifford, D., England, J. R., & Raison, R. J. (2015). Guidelines for Constructing Allometric Models for the Prediction of Woody Biomass: How Many Individuals To Harvest? *Ecosphere*, 6(3), 1–27. https://doi.org/10.1890/ES14-00251.1

Roxburgh, S. H., Wood, S. W., Mackey, B. G., Woldendorp, G., & Gibbons, P. (2006). Assessing the Carbon Sequestration Potential of Managed Forests: A Case Study from Temperate

Australia. *Journal of Applied Ecology*, 43(6), 1149–1159. https://doi.org/10.1111/j.1365-2664.2006.01221.x

Ruark, G. A., Martin, G. L., & Bockheim, J. G. (1987). Comparison of Constant and Variable Allometric Ratios for Estimating *Populus tremuloides* Biomass. *Forest Science*, 33(2), 294–300. https://doi.org/10.1093/forestscience/33.2.294

Srinivasan, S., Popescu, S., Eriksson, M., Sheridan, R., & Ku, N.-W. (2015). Terrestrial Laser Scanning as an Effective Tool to Retrieve Tree Level Height, Crown Width, and Stem Diameter. *Remote Sensing*, 7(2), 1877–1896. https://doi.org/10.3390/rs70201877

Schikowski, A. B., Corte, A. P. D., Ruza, M. S., Sanquetta, C. R., & Montaño, R. A. N. R. (2018). Modeling Of Stem Form and Volume Through Machine Learning. *Anais Da Academia Brasileira de Ciências*, 90(4), 3389–3401. https://doi.org/10.1590/0001-3765201820170569

Schimel, D. (2014). Forests in the Global Carbon Cycle. In T. Fenning (Ed.), *Challenges and Opportunities for the World's Forests in the 21st Century* (Vol. 81, pp. 231–239). Springer Netherlands. https://doi.org/10.1007/978-94-007-7076-8_10

Sills, E. O., Atmadja, S. S., de Sassi, C., Duchelle, A. E., Kweka, D. L., Resosudarmo, I. A. P., & Sunderlin, W. D. (n.d.). *A case book of subnational initiatives across the globe.*

Spurr, S.H. 1952. *Forest Inventory*. Ronald Press, New York.

Srinivasan, S., Popescu, S. C., Eriksson, M., Sheridan, R. D., & Ku, N.-W. (2014). Multi-Temporal Terrestrial Laser Scanning for Modeling Tree Biomass Change. *Forest Ecology and Management*, 318, 304–317. https://doi.org/10.1016/j.foreco.2014.01.038

Srinivasan, S., Popescu, S., Eriksson, M., Sheridan, R., & Ku, N.-W. (2015). Terrestrial Laser Scanning as an Effective Tool to Retrieve Tree Level Height, Crown Width, and Stem Diameter. *Remote Sensing*, 7(2), 1877–1896. https://doi.org/10.3390/rs70201877

Stovall, A. E. L., Anderson-Teixeira, K. J., & Shugart, H. H. (2018). Assessing Terrestrial Laser Scanning for Developing Non-destructive Biomass Allometry. *Forest Ecology and Management*, 427, 217–229. https://doi.org/10.1016/j.foreco.2018.06.004

Stovall, A. E. L., Vorster, A., Anderson, R., & Evangelista, P. (2023). Developing Non-Destructive Species‐Specific Tree Allometry with Terrestrial Laser Scanning. *Methods in Ecology and Evolution*, 14(1), 280–290. https://doi.org/10.1111/2041-210X.14027

Stovall, A. E. L., Vorster, A. G., Anderson, R. S., Evangelista, P. H., & Shugart, H. H. (2017). Non-Destructive Aboveground Biomass Estimation of Coniferous Trees Using Terrestrial LiDAR. *Remote Sensing of Environment*, 200, 31–42. https://doi.org/10.1016/j.rse.2017.08.013

Sumnall, M., Peduzzi, A., Fox, T.R., Wynne, R.H., Thomas, V.A., 2016. Analysis Of a Lidar Voxel-Derived Vertical Profile At The Plot and Individual Tree Scales for the Estimation of Forest Canopy Layer Characteristics. *Int. J. Remote Sens*. 37, 2653–2681. https://doi.org/10.1080/01431161.2016.1183833.

Temesgen, H., Affleck, D., Poudel, K., Gray, A., & Sessions, J. (2015). A Review of the Challenges and Opportunities in Estimating Above Ground Forest Biomass Using Tree-Level Models. *Scandinavian Journal of Forest Research*, 1–10. https://doi.org/10.1080/02827581.2015.1012114

Telfer, E. S. (1969). Weight–Diameter Relationships for 22 Woody Plant Species. *Canadian Journal of Botany*, 47(12), 1851–1855. https://doi.org/10.1139/b69-271

Ter-Mikaelian, M. T., & Korzukhin, M. D. (1997). Biomass Equations for Sixty-Five North American Tree Species. *Forest Ecology and Management*, 97(1), 1–24. https://doi.org/10.1016/S0378-1127(97)00019-4

Thies, M., Pfeifer, N., Winterhalder, D., & Gorte, B. G. H. (2004). Three-Dimensional Reconstruction of Stems for Assessment of Taper, Sweep and Lean Based on Laser Scanning of Standing Trees. *Scandinavian Journal of Forest Research*, 19(6), 571–581. https://doi.org/10.1080/02827580410019562

Tigges, J., Lakes, T., & Hostert, P. (2013). Urban Vegetation Classification: Benefits of Multitemporal RapidEye Satellite Data. *Remote Sensing of Environment*, 136, 66–75. https://doi.org/10.1016/j.rse.2013.05.001

TreesQSM Version 2.4.1 Manual, 2022. https://github.com/InverseTampere/TreeQSM/blob/master/Manual/TreeQSM_documentation.pdf , Last Accessed: 2024-08-19.

T. Vashum, K. (2012). Methods to Estimate Above-Ground Biomass and Carbon Stock in Natural Forests—A Review. *Journal of Ecosystem & Ecography*, 02(04). https://doi.org/10.4172/2157-7625.1000116

UNFCCC (2015). *Measurements for Estimation of Carbon Stocks in Afforestation and Reforestation Project Activities under the Clean Development Mechanism: A Field Manual*

United Nations Framework Convention on Climate Change. (2015). *The Paris Agreement*.

U.S. Forest Service. (2023). Future of America's Forest and Rangelands: Forest Service 2020 Resources Planning I Assessment (WO-GTR-102; p. WO-GTR-102). U.S. Department of Agriculture, Forest Service. https://doi.org/10.2737/WO-GTR-102

Van Breugel, M., Ransijn, J., Craven, D., Bongers, F., & Hall, J. S. (2011). Estimating Carbon Stock in Secondary Forests: Decisions and Uncertainties Associated with Allometric Biomass Models. *Forest Ecology and Management*, 262(8), 1648–1657. https://doi.org/10.1016/j.foreco.2011.07.018

Van Den Broeck, W. A. J., Terryn, L., Cherlet, W., Cooper, Z. T., & Calders, K. (2023). Three-Dimensional Deep Learning for Leaf-wood Segmentation of Tropical Tree Point Clouds. The International Archives of the Photogrammetry, *Remote Sensing and Spatial Information Sciences*, XLVIII-1/W2-2023, 765–770. https://doi.org/10.5194/isprs-archives-XLVIII-1-W2-2023-765-2023

Vorster, A. G., Evangelista, P. H., Stovall, A. E. L., & Ex, S. (2020). Variability and Uncertainty in Forest Biomass Estimates From the Tree to Landscape Scale: The Role of Allometric Equations. *Carbon Balance and Management*, 15(1), 8. https://doi.org/10.1186/s13021-020-00143-6

Weiskittel, A. R., MacFarlane, D. W., Radtke, P. J., Affleck, D. L. R., Temesgen, H., Woodall, C. W., Westfall, J. A., & Coulston, J. W. (2015). A Call to Improve Methods for Estimating

Tree Biomass for Regional and National Assessments. *Journal of Forestry*, 113(4), 414–424. https://doi.org/10.5849/jof.14-091

West, G. B., Brown, J. H., & Enquist, B. J. (1999). A General Model for the Structure and Allometry of Plant Vascular Systems. *Nature*, 400(6745), Article 6745. https://doi.org/10.1038/23251

West, P. W. (2015). Tree and Forest Measurement. *Springer International Publishing*. https://doi.org/10.1007/978-3-319-14708-6

Wilkinson, M. D., Dumontier, M., Aalbersberg, Ij. J., Appleton, G., Axton, M., Baak, A., Blomberg, N., Boiten, J.-W., Da Silva Santos, L. B., Bourne, P. E., Bouwman, J., Brookes, A. J., Clark, T., Crosas, M., Dillo, I., Dumon, O., Edmunds, S., Evelo, C. T., Finkers, R., … Mons, B. (2016). The FAIR Guiding Principles for Scientific Data Management and Stewardship. *Scientific Data*, 3(1), 160018. https://doi.org/10.1038/sdata.2016.18

Yang, M., Zhou, X., Liu, Z., Li, P., Tang, J., Xie, B., & Peng, C. (2022). A Review of General Methods for Quantifying and Estimating Urban Trees and Biomass. *Forests*, 13(4), 616. https://doi.org/10.3390/f13040616

Ye, N., van Leeuwen, L., & Nyktas, P. (2019). Analysing the Potential of UAV Point Cloud as Input in Quantitative Structure Modelling for Assessment of Woody Biomass of Single Trees. *International Journal of Applied Earth Observation and Geoinformation*, 81, 47–57. https://doi.org/10.1016/j.jag.2019.05.010

Yoshimura, T., & Suzuki, Y. (2019). *Evaluating the precision and accuracy of low-cost Global Navigation Satellite System (GNSS) receivers beneath a forest canopy positioned in a crisscross arrangement*

Zhang, Q., Wang, C., Wang, X., & Quan, X. (2009). Carbon Concentration Variability of 10 Chinese Temperate Tree Species. *Forest Ecology and Management*, 258(5), 722–727. https://doi.org/10.1016/j.foreco.2009.05.009

Zhu, R., Guo, Z., & Zhang, X. (2021). Forest 3D Reconstruction and Individual Tree Parameter Extraction Combining Close-Range Photo Enhancement and Feature Matching. *Remote Sensing*, 13(9), 1633. https://doi.org/10.3390/rs13091633s